



University of Tennessee, Knoxville

TRACE: Tennessee Research and Creative Exchange

Masters Theses

Graduate School

5-2001

Spunbonding studies with polypropylene polymers

Ramaiah Kotra

Follow this and additional works at: https://trace.tennessee.edu/utk_gradthes

Recommended Citation

Kotra, Ramaiah, "Spunbonding studies with polypropylene polymers. " Master's Thesis, University of Tennessee, 2001.
https://trace.tennessee.edu/utk_gradthes/9663

This Thesis is brought to you for free and open access by the Graduate School at TRACE: Tennessee Research and Creative Exchange. It has been accepted for inclusion in Masters Theses by an authorized administrator of TRACE: Tennessee Research and Creative Exchange. For more information, please contact trace@utk.edu.

To the Graduate Council:

I am submitting herewith a thesis written by Ramaiah Kotra entitled "Spunbonding studies with polypropylene polymers." I have examined the final electronic copy of this thesis for form and content and recommend that it be accepted in partial fulfillment of the requirements for the degree of Master of Science, with a major in Textiles, Retail, and Consumer Sciences.

Gajanan Bhat, Major Professor

We have read this thesis and recommend its acceptance:

Larry Wadsworth, Kermit Duckett

Accepted for the Council:

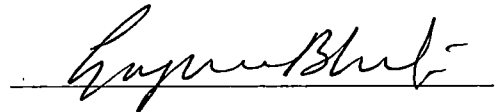
Carolyn R. Hodges

Vice Provost and Dean of the Graduate School

(Original signatures are on file with official student records.)


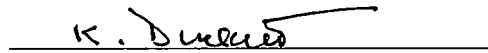
To the Graduate Council:

I am submitting a thesis written by RAMAIAH KOTRA entitled "SPUNBONDING STUDIES WITH POLYPROPYLENE POLYMERS." I have examined the final copy of this thesis for form and content and recommend that it be accepted in partial fulfillment of the requirements for the Master of Science with a major in Textiles, Retailing and Consumer Sciences.



Gajanan Bhat, Major Professor

**I have read this thesis
and recommend its acceptance:**


Larry Wadsworth
Kermit Duckett

Accepted for the Council:



Associate Vice Chancellor

and Dean of the Graduate School

SPUNBONDING STUDIES WITH POLYPROPYLENE POLYMERS

A

Thesis Presented

For the

Master of Science Degree

THE UNIVERSITY OF TENNESSEE, KNOXVILLE, TN.

Ramaiah Kotra

May 2001

DEDICATION

**This thesis is dedicated to
The Mother and Sri Aurobindo,
to my parents
Mr. K. Chitambaraiah and Mrs. K. Lakshmiddevamma
and to my family members and friends.**

ACKNOWLEDGEMENTS

I sincerely thank my major professor and advisor, Dr. Gajanan Bhat, for his guidance, support and encouragement throughout my studies at the University of Tennessee. I would like to thank my other committee members Dr. Kermit Duckett and Dr. Larry Wadsworth for their suggestions and support.

Sincere thanks to Garry Wynn and Jack Wyrick at TANDEC for their help in producing the samples.

Sincere appreciation is extended to other professors and department members of the Textile Science for their help and advice.

Grateful acknowledgements to all my colleagues and friends who helped me and made my study life more interesting and enjoyable.

I am indebted to my parents and family members for their love, support and encouragement in every step of my life.

ABSTRACT

Spunbonding is a continuous process to produce polymer laid nonwovens for various applications. Polypropylene is the major polymer used in this process. Metallocene polypropylene (mPP) manufactured using the single site catalyst technology has been of interest for this industry and some research has been done for the past few years. This polymer seems to be different compared to the conventional Ziegler-Natta catalyzed polypropylene (znPP). This research was conducted to investigate the structure and properties of the filaments and fabrics produced with a metallocene catalyzed propylene polymer and to determine the optimum process conditions to produce good quality fabrics.

A comparison is also made between the filaments and the fabrics produced from both types of polymers i.e., mPP and znPP. An investigation of the processing behavior of mPP polymer was conducted using the Reicofil spunbonding pilot line at the University of Tennessee, Knoxville. The filaments at three different throughput rates were studied for tensile properties and other structural features such as birefringence, x-ray diffraction and thermal responses. The fabrics bonded at different process conditions were tested for various mechanical properties. The structure and properties of the two types of spunbond filaments and fabrics were compared. The failure mechanism of the fabrics at different bonding temperatures was studied using scanning electron microscope.

The results showed that mPP filaments have lower melting temperature than znPP filaments. They also have higher strengths and lower elongation than znPP filaments. The

mPP fabrics also have shown higher strength and elongation properties than the comparable znPP fabrics. The rupture mechanism of the mPP fabrics was found to be different than that of the znPP fabrics. Also higher strength and elongation were observed in mPP fabrics that were bonded at relatively lower temperatures. For spunbonding process mPP was found to be much better than the znPP polymer.

TABLE OF CONTENTS

<u>CHAPTER</u>	<u>PAGE</u>
1. INTRODUCTION	01
2. SPUNBONDING PROCESS	
2.1 Spunbonded Nonwovens: Now and Then	03
2.2 Spunbonding Process	04
2.2.1 Filament Spinning, Drawing and Deposition System	05
2.3 Bonding	07
2.4 Thermal Point Bonding and Effect of Bonding Variables	08
2.4.1 Effect of Bonding Temperature	08
2.4.2 Effect of Calender Nip Pressure	10
2.4.3 Effect of Residence Time	10
2.4.4 Effect of Bond Area	11
2.5 Effect of Process Variables and Material Variables on Properties	11
2.5.1 Effect of Polymer Throughput rate	12
2.5.2 Effect of Polymer Melt Temperature	12
2.5.3 Effect of Primary Air Temperature	12
2.5.4 Effect of Venturi gap	13
2.5.5 Effect of Basis weight	13
2.5.6 Effect of Suction Speed	13
2.6 Polypropylene	13
2.6.1 Preparation of Polypropylene using ZN Catalysts	14

2.6.2 Physical Properties of Polypropylene	14
2.6.3 Effect of Resin/Polymer Characteristics	15
2.7 Metallocene Polypropylene	16
2.7.1 Key Polymer Attributes	19
2.7.2 Fiber Properties	23
3. EXPERIMENTAL DETAILS	28
3.1 Materials and Processing	28
3.2 Characterization	30
3.2.1 Differential Scanning Calorimetry	30
3.2.2 Thermo-mechanical Analysis	30
3.2.3 Viscosity	32
3.2.4 Fiber Diameter	32
3.2.5 Birefringence	32
3.2.6 Tensile Properties	33
3.2.7 Wide Angle X-ray Diffraction	33
3.2.8 Stiffness/Bending Length	34
3.2.9 Tear Strength	34
3.2.10 Fiber Bundle Orientation	34
3.2.11 Single Bond Test	35
3.2.12 Scanning Electron Microscopy	36
4. RESULTS AND DISCUSSION	37
4.1 Filament Properties	37
4.2 Comparison of Filament Properties of znPP and mPP	43

4.2.1 Polymer Viscosity	43
4.2.2 Fiber Structure	43
4.2.3 Thermal Response	45
4.2.4 Tensile Properties	46
4.3 Fabric Properties	47
4.3.1 Effect of Throughput rate	47
4.3.2 Effect of Fabric Weight	49
4.3.3 Effect of Bonding Conditions	54
4.3.4 Rupture Mechanism	59
4.3.5 Single Bond Test	66
4.3.6 Comparison of Fabric Properties of mPP and znPP	69
5. CONCLUSIONS	72
6. RECOMMENDATIONS FOR FUTURE RESEARCH	74
REFERENCES	75
APPENDICES	79
Appendix 1	80
Appendix 2	81
VITA	85

LIST OF FIGURES

<u>FIGURE No.</u>	<u>PAGE</u>
2.1 Schematic Diagram of the Upgraded Reicofil I Spunbonding Line.	06
2.2 Schematic Diagram of the Thermal Point Bonding Process.	09
2.3 Schematic Diagram showing active sites in znPP and mPP polymers.	18
2.4 Schematic Diagram showing the Molecular Weight Distribution.	21
2.5 Fiber diameter as a function of Relative Draw Force.	24
2.6 Birefringence of fibers as a function of Take-up Speed.	26
3.1 Schematic diagram of Process design and Process Variables used in this study.	29
3.2 Schematic of the Single Bond Strip Test.	35
4.1 DSC Scans of the unbonded filaments at different throughput Rates.	38
4.2 X-ray Diffraction patterns of filaments produced at different Throughputs.	40
4.3. WAXD Scans of the Filaments at different Throughput rates.	41
4.4. TMA Scans of Unbonded filaments at different throughputs.	42
4.5. Shear Viscosity of znPP and mPP polymers.	44
4.6. DSC Scans of the filaments produced at 0.43 ghm.	44
4.7. TMA Scans of the filaments produced at 0.43 ghm.	45
4.8. Peak Strength in MD with increasing throughput and 110°C bonding temperature.	48

4.9. Peak Strength in MD with an increasing throughput and 140°C bonding temperature.	50
4.10. Tear Strength in MD with an increasing throughput and 120°C bonding temperature.	50
4.11. Tear Strength in MD with an increasing throughput and 140°C bonding temperature.	51
4.12. Bending Rigidity in MD with increase in throughput and 120°C bonding temperature.	51
4.13. Peak Strength with increasing Fabric weights and 120°C bonding temperature.	53
4.14. Peak Strength with increasing Fabric weights and 140°C bonding temperature.	53
4.15. Tear Strength in MD with increasing Fabric weights and 110°C bonding temperature.	54
4.16. Tear Strength in MD with increasing Fabric weights and bonding temperatures at 0.24 throughput.	54
4.17. Bending Rigidity in MD with increasing fabric weight and bonding temperatures at 0.24 throughput.	55
4.18. Peak Strength in MD with increasing bonding temperatures.	57
4.19. Peak Elongation in MD with increasing bonding temperatures.	57
4.20. Tear Strength in MD with increasing bonding temperatures.	58
4.21. WAXD scans of the filaments.	60
4.22. WAXD Scans of Filaments Produced at 0.43ghm/35g/m ² /140°C.	61
4.23. SEM pictures at 0.24ghm throughput, 20g/m ² basis weight, Group-a.	63
4.24. SEM pictures at 0.24ghm throughput, 20g/m ² basis weight, Group-b.	64

4.25. SEM pictures at 0.24ghm throughput, 20g/m ² basis weight, Group-c.	65
4.26. Load-Elongation curves at different temperatures of fabrics produced at 0.24ghm throughput and 20g/m ² basis weight.	68
4.27. Peak strength of znPP and mPP fabrics in MD produced at 0.24 throughput rate, 35g/m ² basis weight with increasing bonding temperatures.	70
4.28. Peak elongation of znPP and mPP fabrics in MD produced at 0.24 throughput rate, 35g/m ² basis weight with increasing bonding temperatures.	70

LIST OF TABLES

<u>TABLE No.</u>	<u>PAGE</u>
3.1 Parameters of Process Variables.	31
3.2 Identification of the Samples.	31
4.1 Filament Structural Features.	38
4.2. Filaments Tensile Properties.	42
4.3. Comparison of Properties of the Filaments.	46
4.4. Single bond strengths of various groups of fabrics.	67

CHAPTER I

INTRODUCTION

The spunbonding process falls under the general classification of polymer laid nonwoven fabrics. It is based on melt spinning technique and has many similarities to it. The spunbonding process involves many operating, and material variables. A primary factor in the production of spunbonded fabrics is the control of four simultaneous, integrated operations: filament extrusion, drawing, lay-down and bonding.

By manipulating operational and the material variables like polymer type, polymer additives, molecular weight distribution etc., one can produce a variety of spunbonded fabrics with desired properties. In recent years there has been considerable interest in this area from both commercial and scientific point of view [1]. In the past decade, the use of isotactic polypropylene (iPP) dominated the production of spunbond nonwovens. The reasons are its high strength to weight ratio, rheological properties and cost effectiveness [2].

In polyolefin (polypropylene and polyethylene) manufacturing, the monomers are converted to polymers using a catalyst. All catalysts have reactive sites enabling them to perform their function, i.e., linking individual molecules to form a polymeric chain. Conventional catalysts- like Ziegler-Natta (ZN), which is used in the manufacture of PP, are of multi-site. Their sites are different and consequently a range of different molecules are formed during the polymerization. By contrast, the new catalyst system, metallocene catalysts have only one reactive site and there by reduce the differences between

individual polymer molecules [3]. This increased homogeneity of the polymer leads to controlled molecular structure and a narrow molecular weight distribution, which allows for finer fiber extrusion. This in turn enables spunbonders to create nonwovens with a more 'cloth-like' handle [4]. The metallocene PP (mPP) manufacturers also claim many advantages such as improved strength of nonwovens, a wider range of melt points (120-164°C), improved yields, reduced extractable content, reduced equipment downtime and no noticeable odor [5, 6]. However, despite their numerous advantages, the relatively higher price of metallocenes make them economically feasible only for high-performance (polyolefins) applications. The other limitations of metallocene polymers are processability. Single-site metallocene catalysts yield resins with very narrow molecular weight distributions (MWD), but make them more viscous. So, they need more time and energy for processing [7]. However, there is increasing need for process optimization to realize the full potential of this new polymer.

This research was conducted to investigate:

1. The structure and properties of the filaments and their influence on fabric properties produced with a metallocene catalyzed propylene polymer (mPP), and to predict the optimum process conditions.
2. The failure mechanism of fabrics produced at different process conditions and to compare the properties of filaments and fabrics produced with metallocene and ZN catalyzed polypropylenes.

To achieve the objectives, several tests were conducted on the unbonded filaments and fabrics. The results were compared with the results of fabrics produced using znPP and reported earlier [8]. The rupture mechanism was observed under a SEM.

CHAPTER II

SPUNBONDING PROCESS

2.1 Spunbond nonwovens: Now and Then

Spunbonds, which are made of continuous filaments, are considered a unique class of materials within the general category of nonwovens. Spunbond is a fabric formed from continuous filaments that are extruded, drawn, laid into a fiber web on a collecting belt, conveyed to a station where the fibers are bonded together by various methods, and collected in roll goods form, all steps being done on a single, integrated process line [9]. Spunbonds are distinguished from other nonwovens in their one-step manufacturing process. Commercialization of this process dates to early 1960's in U.S.A and Western Europe, and the early 1970's in Japan [10].

Although spunbonding began to emerge about 30 years ago, it has experienced its most dramatic evolution in the past decade. The current growth rate for spunbonded nonwovens is in the order of 6-8% per year [10]. Spunbond fabrics are made from a wide range of polymers, including polyethylene, polypropylene, polyester, nylon and combination there of, for example, either bicomponent fibers or the use of two different fibers in the same fabric structure. Each polymer system has its own combination of physical and chemical characteristics. Because of this, each polymer system is chosen to be made into fabrics for specific applications. Nylon and polyester fabrics are generally used in applications where strength is important and higher temperatures are encountered, while the polyolefins are used in applications where softness is the criterion [9].

Uses for spunbonded fabrics can be segmented into disposable and durable categories, both of which include markets that are usually large and constant in demand. On the disposable end, the most influential end use for spunbonds is the baby diaper market, where spunbonded fabrics are used as diaper coverstock. Healthcare applications – including such markets as surgical pack items and medical apparel – are another important disposable end use for spunbond nonwovens.

As for durable end uses, significant areas of growth include filtration, and building and construction industries, where spunbonds are used in geotextiles and roofing membranes. Growth has also been achieved in automotive primary carpet backing and carpet tiles, where spunbonds offer moldability and high dimensional stability.

Future competition for existing spunbonded markets is expected to come from film, foam or advances in alternative technologies within specific market segments. For the future, spunbonded nonwovens are expected to thrive, as consumption in both durable and disposable areas continues to grow [10].

2.2 Spunbonding process

The spunbonding process consists of four integrated operations: filament extrusion, drawing, lay down and bonding. The entire process is a continuous one. In the initial spinning process the fiber-forming polymer is melted and extruded through a block of spinnerets to produce a curtain of filaments. One of the three generic spinning techniques, melt spinning, dry spinning or wet spinning, is employed in a spunbonding process. The drawing of the filaments follows the spinning. In conventional fiber spinning, drawing of the filaments is achieved using draw rollers. While, in a

spunbonding process it is achieved using a specially designed aerodynamic device [1]. The filament deposition follows the drawing. The aerodynamic devices also aid in entangling the filaments and random laydown on the conveyor belt [11]. The conveyor belt carries the unbonded web to the bonding zone. Among the various bonding techniques, thermal bonding is the most widely used one. The bonding is achieved by fusing of the filaments in the web at the crossover points [1]. Finally, the spunbond web is wound on a cardboard core and processed further according to the end-use requirements.

2.2.1 Filament Spinning, Drawing and Deposition system

Over the past twenty-five years many filament spinning, drawing and deposition systems have been patented and commercialized. 'Docan' and 'Reicofil[®]' are some of the successful systems. The Reicofil system was developed by Reifenhauser GmbH of Germany and is based on the melt spinning technique [1]. A schematic diagram of the modified Reicofil I spunbonding system at the TANDEC Laboratory is shown in figure 2.1. The extruding and quenching have been upgraded from the Reicofil I system. The melt is forced by spin pumps through special spinnerets or die block. The diameter of the spinneret holes is 0.6mm. The blow ducts located below the spinneret block continuously cool the filaments with conditioned air. Over the line's entire working width, a ventilator generated under-pressure sucks filaments and air down from the spinnerets and cooling chambers. The filaments are sucked through a venturi, which is a high-velocity, low-pressure zone, to a distributing chamber, which affects fanning and entanglement of the filaments. Finally, the entangled filaments are deposited as a random web on a moving

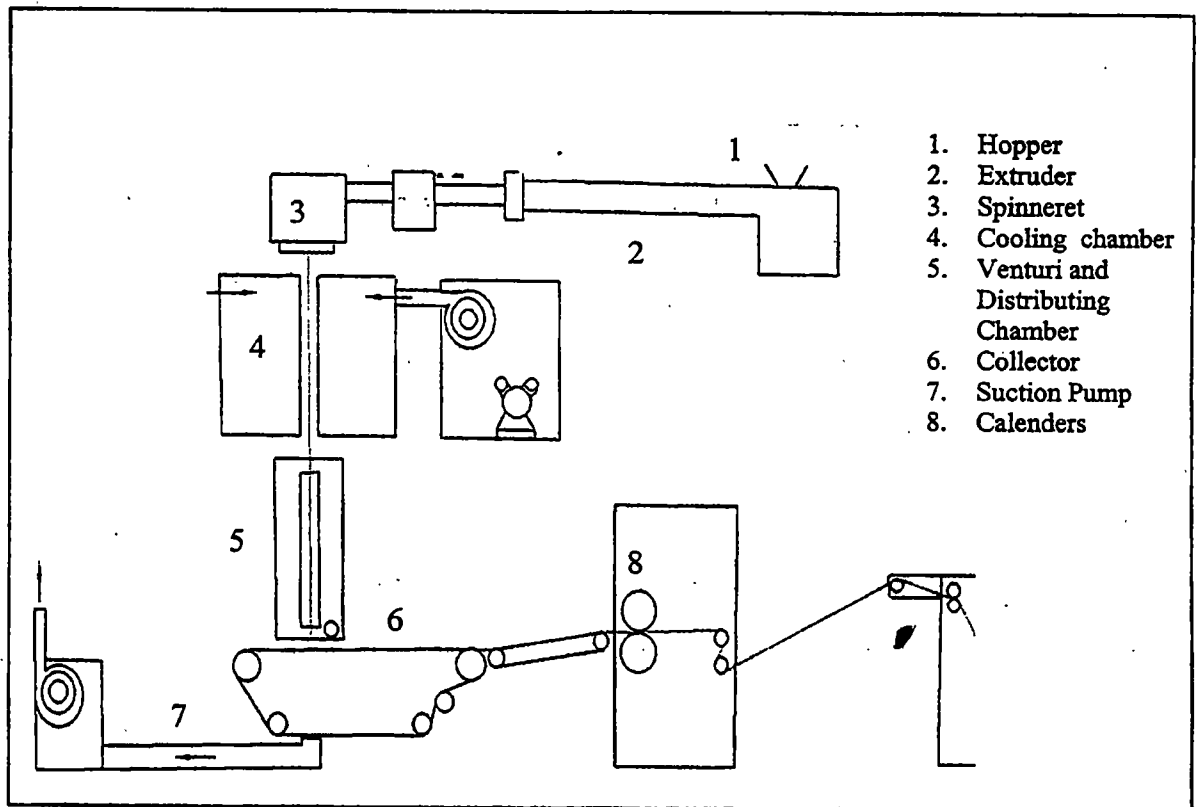


Figure 2.1. Schematic Diagram of the Upgraded Reicofil I Spunbonding Line [1].

sieve belt. Suction below the belt enhances the random laydown of the filaments, which is primarily due to the air turbulence in the distributing chamber [1].

2.3 Bonding

There are three basic bonding techniques employed in a spunbond process: thermal, chemical/adhesive, and mechanical. Spunbond fabrics are receptive to various bonding techniques and can be made from a variety of fibers having different polymer composition and fiber diameters. They are therefore able to be designed to serve numerous application requirements. While bonding of the individual filaments to form a unified web is necessary to produce a fabric having strength properties, each of the various bonding techniques has advantages and disadvantages. Unfortunately, it is unrealistic to make comparisons between bonding of different fabrics because of the variations in polymer characteristics and fiber diameters [9]. The choice of a particular bonding technique is dictated mainly by the ultimate fabric applications. However, thermal bonding is the most prevalent method of bonding in use in nonwovens industry since it offers high production rates and also is suitable for various types of fibers. The bonding is achieved by fusion of the filaments in the web at the crossover points. The fusion is achieved by the direct action of heat and pressure via a calendar. Many of the web qualities depend on the degree of interfiber fusion and bonding [1].

The thermal bonding process can be divided into two types:

- a. Area bonding: The bonding is achieved by passing the web through a pair of heated and smooth calendars. This bonds the entire surface area. The products tend to be stiffer and more paper-like in appearance.

b. Point bonding: The bonding is achieved in a small fraction of the total surface with the aid of an engraved calendar and smooth calendar. Since point bonding can be accomplished with as little as 10% bonding area, such webs are considerably softer and more textile-like in handle [1, 12].

2.4 Thermal point bonding and effect of bonding variables

The largest volume of thermal bonded spunbond fabrics is represented by the ubiquitous point bonded materials [9]. The process is shown in figure 2.2. The unbonded fiber web consisting of thermoplastic fibers is conveyed into the nip of heated engraved steel roller and a heated smooth steel roller. The residence time in the nip is about 10ms, temperature of the rolls is close to the softening point of the polymer and load is of the order of 30 to 300KN/m. The web is compressed under the land areas of the engraved rollers and is also heated. The pressure and heat soften and melt the fibers causing the polymer to flow and create a bond point [13].

The process of thermal point bonding is influenced by many factors. They can be broadly categorized into process related factors, polymer related factors, and fiber related factors. The main variables that can be manipulated to obtain the optimum properties to the fabric are calendar temperature, calendar pressure and the contact time.

2.4.1 Effect of bonding temperature

The effect of calendar temperature on various fabric properties has been studied by a number of researchers. When an unbonded web is passed between calendar rollers

THERMAL POINT BONDING PROCESS

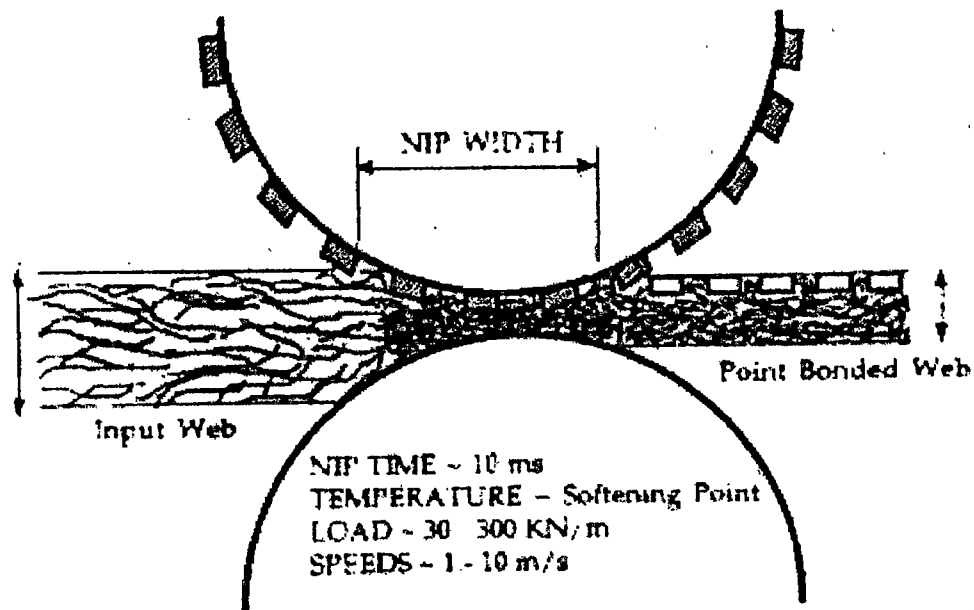


Figure 2.2. Schematic Diagram of the Thermal Point Bonding Process [14].

then it is heated by contact and also compressed due to the calendar pressure. Transmission of heat into the web is mostly due to conduction. Several researchers have modeled the temperature profile across the thickness of the web [15, 16]. DeAngelis *et al.* found that the breaking strength reached a maximum at a critical bonding temperature at constant nip pressure and line speed. Above this critical temperature, the properties deteriorate. The critical bonding temperature was also seen to be a function of the calendering speed at constant nip pressure [17].

2.4.2 Effect of calender nip pressure

Since heat transfer is mainly due to conduction, pressure plays a very important role in this heat transfer. Application of pressure squeezes the air out, increases the fiber-to-fiber and fiber-to-calendar contact. It deforms the fibers at the bond areas causing the polymer to flow and stick, and also causes heating due to deformation. Researchers have reported that the nip pressure does not affect the critical bonding temperature. The maximum strength may be changed depending on the melting behavior of the fibers.

2.4.3 Effect of residence time

Production speed and diameter of the rolls determine the residence time in the nip. The breaking strength is significantly affected by the residence time. It was found that with increased speeds, the calendar temperature had to be increased to obtain the maximum properties. The average area of each bond was seen to reduce with increased production rate and increase with increased pressure. Strength tended to increase with lower bond areas probably because of reduced damage to the fibers. An increase in the

production speed compensated with appropriate increase in calendar temperature reduced the bond area and produced stronger fabrics [14].

2.4.4 Effect of bond area

Earlier studies have shown that the bond area has a great influence on the softness of the fabric. Fewer the individual filaments bonded, the more flexible the fabric as a whole. The effect of bond area on the tensile strength is not as great as one might have expected. Even going to a low bond area of 6% from a totally bonded fabric only reduced the tensile strength by about 20%. On the other hand, tensile elongation greatly increased as the bond area was reduced: going from fully bonded to 6% bond area increased the elongation by 100% or more. The tear strength also increased significantly as the bond area was reduced. The larger number of unbonded filaments allows greater movement in the fabric structure and this increased conformability increases the tear strength [9].

While the major performance characteristics of spunbond fabrics such as strength, and chemical and thermal resistance, are controlled by the characteristics of the polymer system used to produce the fibers, it is also apparent that softness and conformability of the fabrics are highly influenced by the bonding. No matter what polymer or what fiber diameter is used, bonding is capable of contributing significantly to the performance characteristics of spunbond fabrics.

2.5 Effect of process variables and material variables on filament and fabric properties in Spunbonding process

2.5.1 Effect of polymer throughput rate

Sanjiv Malkan and Dong Zhang *et al.* [18, 19] have reported an increase in the final filament diameter as the polymer throughput rate was increased. The primary airflow rate and suction speeds were increased in order to balance the air-to-polymer ratio. Increase in diameter was attributed to lower drawdown, increased die swell and slower cooling along the spinline. The bonded web breaking strength decreased with increase in throughput rate, which can be attributed to morphological differences of the filaments [18].

2.5.2 Effect of polymer melt temperature

Increase in polymer melt temperature resulted in a decrease in filament diameter since the drawing force required to draw down melts of higher temperature is less. But, the change in diameters was modest [10]. Higher melt temperature tends to degrade the polymer producing filament breaks and spots on the spinbelt. Using lower melt temperature causes difficulty in drawing due to higher polymer viscosity.

2.5.3 Effect of primary air temperature

Filament diameter decreased with increase in primary air temperature, keeping all the other variables constant. The decrease was mainly due to slower cooling of the extruded filaments, and slower crystallization occurring much further from the spinneret [18]. With increase in air temperature, the viscosity remains at a lower value for a longer time after extrusion and hence the filament diameter reduces.

2.5.4 Effect of Venturi gap

The venturi gap controls the uniformity of laydown of the filaments. Visual examination of the bonded webs showed that at lower venturi gap the webs were non-uniform than with high venturi gap. Lower gap with higher cabin pressure causes more oscillations and instabilities to filament streams, which in turn produces a non-uniform web structure. Breaking stress of the webs increased with increase in venturi gap for the same reason [18].

2.5.5 Effect of Basis weight

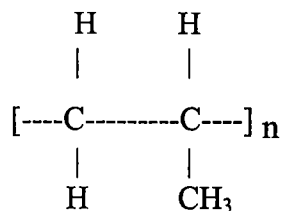
Filament diameter increased with increasing basis weight with all other variables remaining constant. The increase was due to the fact that at higher basis weights the effectiveness of the suction is reduced due to the reduced porosity of the web. This has an effect of reducing the drawdown of the filaments [18].

2.5.6 Effect of Suction speed

The role of suction speed is to attenuate the filaments. Increase in suction speed increases the drawdown of the filaments and hence leads to finer filaments.

2.6 Polypropylene

Polypropylene was first polymerized in the mid 1930's, but it was not until the preparation of isotactic polypropylene utilizing the Ziegler-Natta (ZN) catalysts that the resin was fully exploited. The chemical structure of polypropylene is shown below



2.6.1 Preparation of polypropylene using Ziegler-Natta (ZN) catalysts

Preparation of PP involves preparation of catalyst, polymerization, purification, solvent recovery and compounding. The monomers are reacted using a catalyst. The previous breakthrough in polyolefin synthesis had been the ZN catalyst, commonly titanium trichloride on a magnesium chloride support. These catalysts have many reactive sites located randomly on the surface of the catalyst. These produce isotactic polymers with a crystalline structure and also eliminate some of the disadvantages of earlier catalysts. However, these catalysts produce different and varying polymers due to many reactive sites i.e., one site will produce highly isotactic polypropylene and the others will produce atactic polypropylene [20].

2.6.2 Physical properties of Polypropylene

Polypropylene is a white semicrystalline solid polymer. It is produced with broad range of MFRs to be suitable for various applications. The degree of crystallinity depends on the processing conditions, but usually ranges between 50-65%. The glass transition temperature is -10°C and the melting point is about $160\text{-}170^{\circ}\text{C}$ [14]. The specific gravities of fully crystalline and fully amorphous polypropylene are 0.9363 and 0.8576 respectively. Several important fiber technologies take advantage of the drawability of PP resins. PP provides the highest yield (fiber per kilogram) and covering power at the

lowest cost because of its low density. The main disadvantage of PP is that it degrades in UV light. However, by using stabilizers this property can be greatly improved [1].

Polypropylene exists in three forms: Isotactic, Syndiotactic and Atactic

a. Isotactic PP: It is a stereo specific polymer because the propylene units are added head to tail so their methyl (CH_3) groups are all on the same side of the plane of the polymeric backbone. It crystallizes in a helical form and exhibits good mechanical properties, such as stiffness and tensile strength. Homopolymer has the highest stiffness and melting point of the three types and is marketed in a wide range of melt flow rates.

b. Syndiotactic PP: It is made by inserting the monomer units in an alternate configuration. It lacks the stiffness of the isotactic form, but has better impact and clarity.

c. Atactic PP: It is produced via a random arrangement of the monomer. This form lacks the crystallinity of the other two. It is mainly used in roofing tars and adhesives applications.

Among these, isotactic polypropylene has been used predominantly in commercial production.

2.6.3 Effect of resin/polymer characteristics

The main resin characteristics affecting the extrusion and spinning processes during the production of nonwovens are

a. Melting point: Most of the conventional PP resins melt around 165°C . The melting point directly affects the melt temperature during processing. The higher the melting point, higher the energy requirements.

b. Molecular Weight distribution (MWD): The narrow molecular weight distribution of the resins reduces the melt elasticity and melt strength of the resin so that the melt stream can be drawn into fine denier filaments without excessive draw force. The broad MWD increases melt elasticity and melt strength, which makes fiber drawing difficult, therefore, a broad MWD resin is prone to produce fiber breaks and stiffer webs.

c. Melt viscosity: Melt viscosity is a function of Melt Flow Rate (MFR) and melt temperature. The melt viscosity of the melt has to be appropriate for easy processing.

d. Resin cleanliness: Due to fine diameter of the spinneret holes, it is important to have a resin with practically no contaminants. The contaminants plug up the spinneret holes during processing causing inconsistency in the final product [21].

2.7 Metallocene Polypropylene

Sinn and Kaminsky's discovery of new catalytic systems based on the combination of metallocenes with alkylaluminumoxane started a new era in polyolefins. Metallocene catalyzed polyolefins represent the most significant breakthrough in the polymer industry. Exxon Chemical Company announced the commercialization of metallocene-based isotactic propylene polymers with the trade name ACHIEVE™ in October 1995 [22]. Since then, single-site or metallocene-catalyzed polymer developments have been streaming out of laboratories very fast. Metallocene catalyst technology is being used to enhance and 'tailor' properties of polyolefins, opening up opportunities for value added products with a performance to match. Several industry experts feel that metallocenes have the potential to affect the polypropylene industry as significantly as they have influenced polyethylene. They feel that metallocene propylene

polymers are expected to increase the size of the global market for polypropylene by around 45 per cent [4].

Metallocene catalysts offer polyolefin producers an ability to control polymer chain length, branching and tacticity [20]. They are found to be very different from the conventional Ziegler-Natta catalyzed polypropylenes. The differences in the behavior between the two types of resins are suggested to be a result of the differences in molecular microstructure of the resins. Characterization of the molecular structure suggest that the mPP resins have a more uniform defect distribution from chain to chain, compared to the znPP. The results have suggested that the Ziegler-Natta catalysts have more than one type of active site, perhaps as many as three or more. Typically in these mechanisms, one site will produce highly isotactic polypropylene and the others will produce atactic polypropylene [23]. Since metallocenes are single-site catalysts, the reaction sites are virtually identical and therefore produce very uniform polymers as shown in figure 2.3. Therefore, producers can better control polymerization and performance characteristics of individual polymers, tailoring them for niche applications [24, 25].

Compared to conventional heterogeneous catalysts such as the well-established Ziegler-Natta system, the mechanism of metallocene-based catalysts is relatively easy to study because every catalytic site has the same molecular structure. With Ziegler-Natta, the metal is the active site that directs polymerization while the organic portion (ligand)

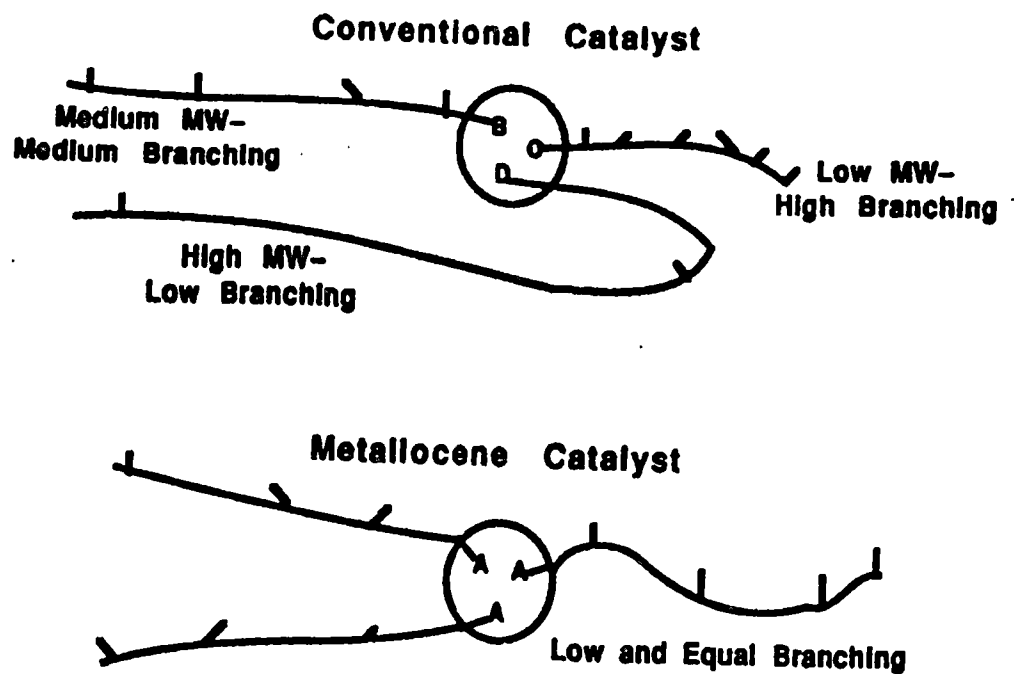


Figure 2.3. Schematic diagram showing active sites in znPP and mPP polymers [21].

modifies the activation energy at the metal. The support also interacts and modifies the activation energy of the metal. The spread of activation energies increases the randomness of the molecular weight of the polymer [26].

On the other hand, metallocene catalysts are transition metals sandwiched between cyclopentadiene rings. Before the metallocene can catalyze the polymerization, it must first react with methylalumoxane (MAO) with which it is mixed. The details of this first step are not yet understood, but somehow the chlorine atoms are removed from the metal atom and the zirconium complex is transformed into a methylated cation. MAO acts as a balancing ion, but the structure of the cation-anion complex has yet to be discovered. It is believed that the polymerization starts in the second step, when the alkyl group moves to a propylene molecule that attaches itself at the chiral metal. In the third step, propylene is inserted into the carbon metal bond. The growing polymer chain moves towards the monomer, which is still attached to the metal. Then the chain and monomer exchange positions and the whole sequence begins again, to give isotactic polypropylene.

2.7.1 Key polymer attributes

Among the key attributes found in the first generation of metallocene-based propylene polymers are narrow molecular weight distribution and composition distribution, lower melting point and low extractables [22]. The mPP resins have very narrow molecular weight distributions, a result of the single site metallocene catalyst system that produces these distributions without viscosity breaking the addition of peroxides. This fact alone, the generation of narrow MWD resins, is a major

breakthrough in catalyst technology that allows custom generation of molecular chains that are similar in length, and as will be shown, tacticity [23].

These properties lead to significant differences in extrusion behavior and fabrication processes as well as end-product properties.

a. Narrow Molecular Weight distribution

For high-speed spunbond nonwoven applications, the MWD of the polymer should be narrow: the narrow MWD polymer has lower melt elasticity and can be spun at higher speeds to achieve finer denier. Being single-sited, propylene polymers produced by the metallocene catalyst have a molecular weight distribution of 2.0 (measured by M_w/M_n). This is in contrast to broad range of MWD of 3-6 for the conventional PP (see figure 2.4). This broad MWD is a result of the multiple active sites of the conventional catalysts [3]. So they must be thermally or chemically broken down in the post-reactor extrusion (a process called Controlled Rheology, or CR process) to obtain a narrow MWD polymer grade suitable for nonwoven applications. This process requires a sophisticated control and monitoring system and operational experience in order to produce a uniform product. However, the metallocene propylene polymers directly offer this narrow MWD and show a more uniform and consistent molecular weight and MWD.

b. Elongational Viscosity and Melt Elasticity

Metallocene propylene polymer exhibits low elongational viscosity than conventional ZN propylene polymer. The low elongational viscosity reduces spin line stress and therefore the polymer can be extended more easily. The low elongational viscosity is also favorable for spinning at a higher line speed. The mPP polymer also has low melt elasticity. This is due to ultra narrow MWD. The low melt elasticity reduces the

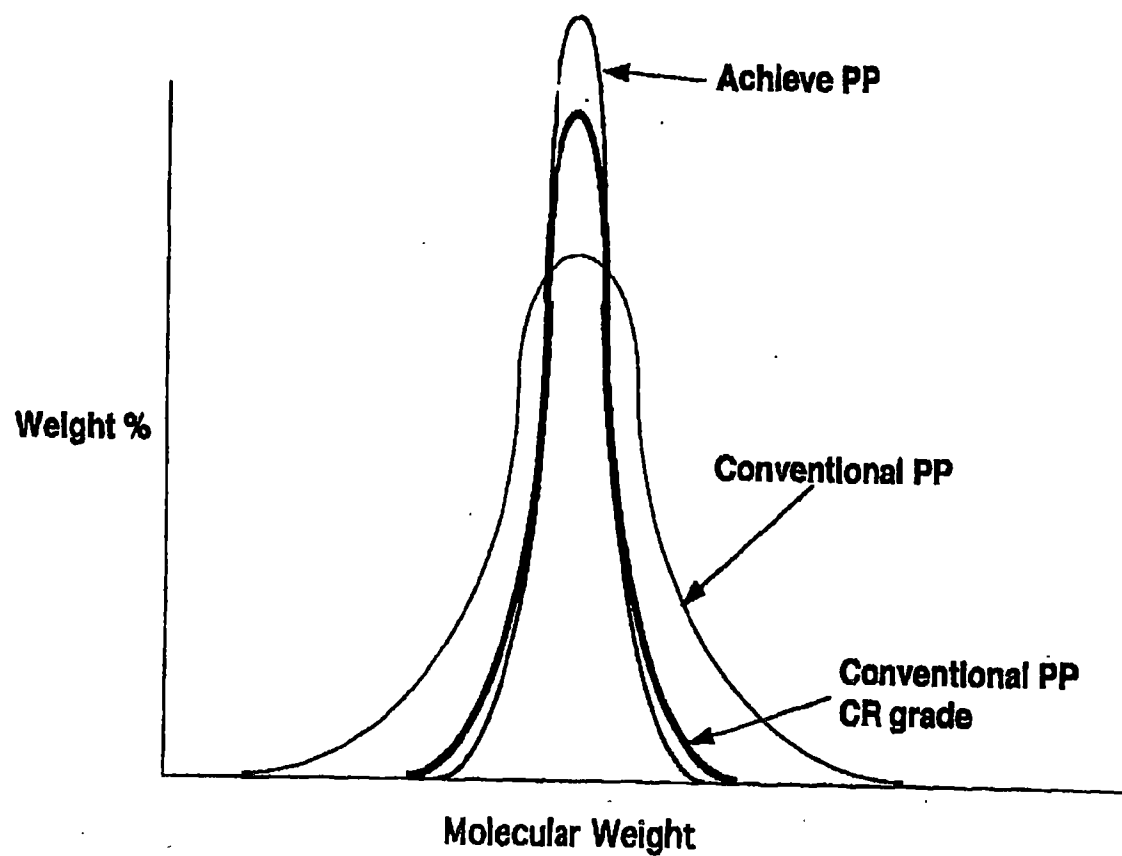


Figure 2.4. Schematic Diagram showing the Molecular Weight Distribution [3].

die swell at the spinneret exit and therefore the effective drawdown ratio is reduced. This improves the spinning continuity and reduces the number of fiber breaks.

c. Thermal properties

Thermal properties of mPP are different from that of znPP due to the degree of crystallinity and type of crystalline structure. The research studies have shown that the isotacticity level is the parameter that most determines the crystallization temperature and melting temperature, as well as crystallinity. The studies on these resins have shown that the catalyst type has an influence on the stereostructure [23]. The occasional reversal of head-to-tail polymer chain growth in mPP also hinders crystalline growth. The peak melting temperature is therefore, lower than that of conventional PP by approximately 8-10°C. The crystalline peak temperature for mPP is generally at 100°C to 101°C compared to the conventional resin at 105°C to 106°C [22].

d. Extrusion characteristics

The melt viscosity for the metallocene resin is higher than that of the conventional polymer of same MFR. Therefore, one can expect viscous shear heating in a plastication extruder to be higher for the metallocene resin. The higher torque and extruder motor amperage load arise from the greater viscous shear heating. The higher energy input into the polymer through viscous shear heating results in higher melt temperatures under similar barrel settings. Although the low shear sensitivity of the narrow MWD mPP results in higher extrusion torque and melt temperature, it does not pose a limitation on extrusion performance. In general, the metallocene PP can be extruded at the same conditions as the conventional PP. However, the melt temperature will be somewhat higher than the conventional resin of the same MFR. A lower barrel temperature setting

of 3°C to 5°C can be used to compensate for higher viscous shear heating by reducing the external heat input at the melting section and increasing cooling at the metering section of the screw [22]. So, it is easier for the processor to convert the polymer usage from conventional to metallocene based grades.

e. Low volatiles and extractables

The metallocene propylene polymers will generate significantly reduced oil and wax deposits and exhibit lower odor. This reduces the fiber breaks and frequency of downtime to remove those waxy deposits and thereby improving the productivity.

f. Spinning

The single-sited metallocene catalyst produces very uniform molecular species. The MW of each polymer chain is very similar (and hence the narrow MWD product). Therefore, there is a very low MW fraction that volatilizes during extrusion. The emission of low molecular species during fiber spinning is practically eliminated for mPP resin. This has a positive long-term impact on productivity (reduced down-time and improved safety) and environmental cleanliness [22].

2.7.2 Fiber Properties

a. Fiber diameter

Under a given draw force, the fiber diameter of mPP resin is smaller than the conventional resin of the same MFR extruding under the same melt temperature. The difference is greater as the draw force is increased. Figure 2.5 compares the fiber size of mPP and znPP [22].

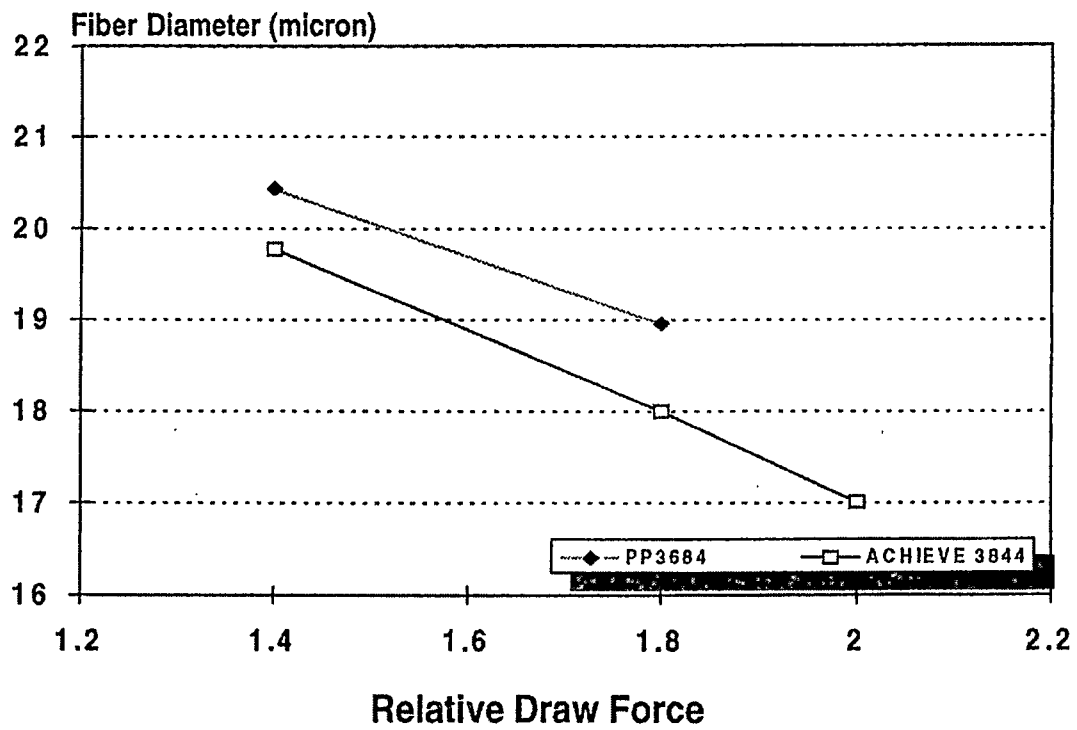


Figure 2.5. Fiber Diameter as a function of Relative Draw Force [3].

b. Fiber Orientation

Molecular orientation in the fiber spinning process is strongly dependent on the spin line stress near the crystallization point. Being able to reach a finer fiber diameter increases the stress near the crystallization region and therefore, molecular orientation is enhanced. The narrow MWD further enhances the tendency of molecular alignment during extensional flow.

Figure 2.6 compares the molecular orientation of mPP and znPP of the same MFR as measured by birefringence. As expected, the differences are greater between the two polymers as the extensional rate increases. The higher molecular orientation leads to higher tenacity and low elongation of the fiber as expected [22].

c. Fiber tensile strength

A narrow MWD polymer can be oriented much more readily than a broader MWD polymer of the same MFR. Therefore, under the same rate of orientation, a metallocene resin will have higher tensile strength than a narrow MWD conventional PP [3].

However, there are differences of opinion about this new polymer. Brookman [22] has suggested that because of the narrow molecular weight distribution, fewer higher molecular weight species, which ordinarily act as melt stiffeners, are present in the metallocene polyolefins. This typically results in lower strength and eventually melt fracture.

Eckstut *et al* [7] summarized the properties of metallocenes. In addition to a lot of advantages offered by the polymer, the following observations were also reported. The metallocene resins are stiffer than the conventional resin; metallocenes are tackier and

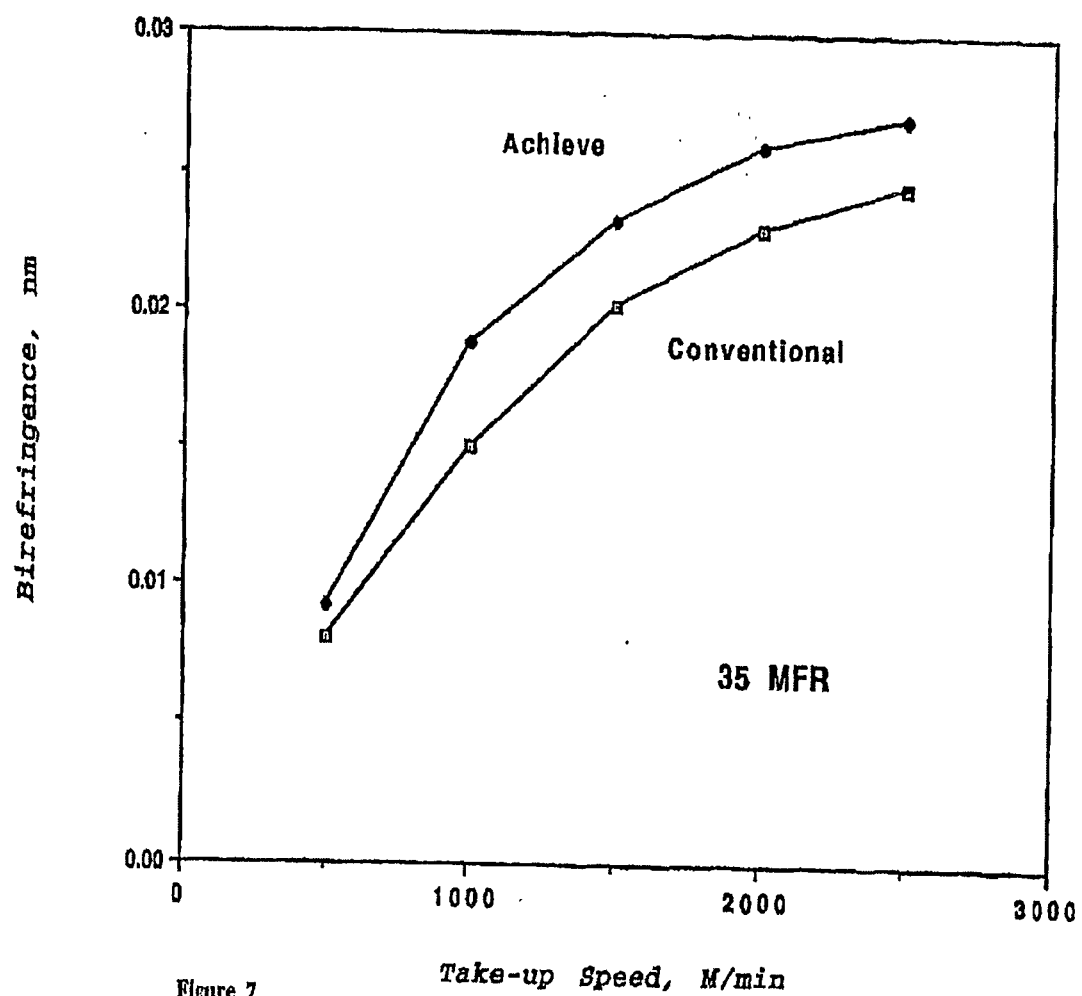


Figure 7

Figure 2.6. Birefringence of fibers as a function of Take-up Speed [3].

may gum up the equipment; 10 to 15% more horse power is required to move resins through equipment; resin have greater shear resulting in lowering of operating temperatures.

CHAPTER III

EXPERIMENTAL DETAILS

3.1 Materials and Processing

The polymer used in this study was a metallocene catalyzed polypropylene (mPP) with 32 MFR and was supplied by the Exxon Chemical Company. Processing was done on the modified Reicofil I spunbonding line at the Textile and Nonwovens Development Center (TANDEC) of the University of Tennessee, Knoxville. The design used was similar to the one used by earlier researcher [8] with ZN catalyzed polypropylene. The spunbond fabrics were produced by varying three process variables namely: polymer throughput rates, web basis weight and web bonding temperature. Three different throughput rates of 0.24, 0.35, and 0.43 ghm were produced. At each throughput, two basis weights of 20 and 35 g/m² were used. However, fabrics of low basis weights (20g/m²) were not produced at the higher throughput of 0.43ghm due to the speed limitation of the collector belt. All fabrics were bonded at four different temperatures and the details are shown in figure 3.1. The bonding temperatures chosen were about 10°C lower to that used for znPP. The reason for this was the lower melting point of mPP reported in the literature [22]. During processing, with increase in throughput rate, air speeds were increased to keep the filament diameter of all the samples in the range of 18 micrometers. The bonding pressure was kept the same for a basis weight and was increased for higher basis weights. The other process conditions were chosen based on suggestions by the machine manufacturer.

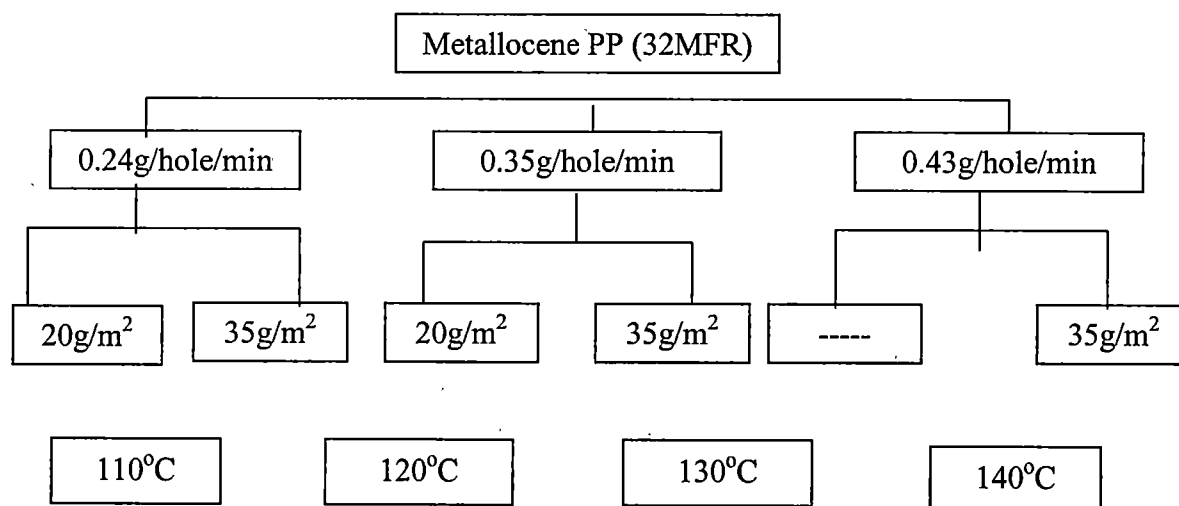


Figure 3.1. Schematic of Process Design and Process Variables used in this study.

The process conditions are listed in table 3.1. The filaments at all throughputs were collected from the conveyor before bonding for testing. The samples produced were then characterized for various mechanical and structural properties. These samples were identified as A-E as shown in table 3.2. In each group, fabrics produced at four bonding temperatures of 110, 120, 130, and 140°C were numbered from 1-4 respectively.

3.2 Characterization

3.2.1 Differential Scanning Calorimetry (DSC):

DSC was carried out on the polymer and the filaments in the presence of air using the Mettler DSC 25. The granules/filaments (approximately 5mg in weight) were sealed in the sample holders and scanned at a rate of 20°C/min from 25°C-300°C. The online computer graphware programs were used to estimate the crystallinity and the melting temperature. Crystallinity was calculated using a ΔH value of 190 J/g for 100% crystalline polypropylene [27]. An average of three scans was used to estimate the crystallinity of filament samples.

3.2.2 Thermo-mechanical Analysis

A filament bundle was made by separating out ten filaments. The filaments were scanned at a heating rate of 10°C/min from 30-200°C. A gauge length of 13mm was used. The samples were tested at two tensions one at low (0.0001N) and another at high tension (0.1N). Finally, the change in length with increase in temperature was recorded.

Table3.1. Parameters of Process Variables.

Throughput (g/hole/min)	0.24	0.35	0.43
Basis weight (g/m ²)	35	35	35
Spin belt speed (mpm)	23.8	34.2	42.6
Cool. Air speed (rpm)	1843	2563	3017
Suction. Air speed (rpm)	1593	2246	2504
Bond Nip Pressure (pli)	253	251	251
Basis weight (g/m ²)	20	20	--
Spin belt speed (mpm)	41.5	61.3	--
Cool. Air speed (rpm)	1851	2542	--
Suction. Air speed (rpm)	1592	2245	--
Bond Nip Pressure (pli)	168	167	--

Calender temperatures: 110, 120, 130, and 140°C for each sample.

Table 3.2. Identification of the Samples.

Throughput rate (g/hole/min)	Basis weight (g/m ²)	Group code
0.43	35	A
0.35	20	B
0.35	35	C
0.24	20	D
0.24	35	E

3.2.3 Viscosity

A steady state viscosity test of both metallocene catalyzed and Ziegler- Natta catalyzed polypropylene resins was carried out on an Advanced Capillary Extrusion Rheometer (ACER 2000), from Rheometric Scientific. The test was carried out over a shear rate range of 10 to 1000 sec^{-1} at 230°C. The test was repeated three times for each polymer.

3.2.4 Fiber diameter

Fiber diameter was measured using the WEBPROTM, an image analysis system developed at the University of Tennessee [28]. An average of 100 readings was taken for each sample. Care was taken during the measurement of bonded webs to make sure that the diameter was not measured very close to a bond area, where the fibers are flattened. The data recorded was checked and readings too large due to errors in filament boundary demarcation were rejected. Filament diameter was also measured using an optical microscope.

3.2.5 Birefringence

Birefringence was measured by the retardation technique using an optical microscope with a compensator. Filaments were carefully separated from the unbonded webs, and laid on a glass slide for measuring the birefringence. The birefringence of the filaments in the unbonded region of the fabrics produced at different throughput rates were also measured using this technique. An average of sixteen readings is reported.

3.2.6 Tensile properties

Filaments and fabric samples were tested on the United tensile tester for tensile properties. A filament bundle was made by carefully separating out five filaments from the unbonded web and was mounted between jaws of the tester with a constant pre-tension. The filaments were tested at a constant rate of extension of 1.27cm/min. The gauge length used was 2.54cm. The fabrics were cut with a template measuring $25.4 \times 2.54 \text{ cm}^2$ ($10 \times 1 \text{ inch}^2$) along the machine direction and the cross direction. The gauge length used was 12.7cm (5 inch) and the extension rate of 12.7 cm/min (5 inch/min) was used for testing. An average of eight readings is reported.

3.2.7 Wide Angle X-ray Diffraction (WAXD)

The Philips flat plate x-ray diffractometer was used to obtain the x-ray photographs of the filaments produced at increasing throughput rates. Samples were prepared by placing a bundle of filaments parallel on a sample holder. The sample was exposed to x-rays at 35kV and 15mA for a time period of six hours. The distance between the film and sample was maintained at 36.5mm.

The Rigaku Geigerflex Diffractometer was used to measure the diffraction in reflection mode. Crystallite sizes were determined for the unbonded filaments, and bonded and unbonded regions of the fabrics. Duco cement was used to hold the samples together. The samples were scanned from $10\text{-}30^\circ$ at a rate of 0.01° for 4 seconds. The reflected intensities were recorded on the attached computer. Results obtained as intensity vs 2θ plots were analyzed using the attached software. Crystal sizes were calculated using the Scherrer equation.

3.2.8 Stiffness/bending length

Stiffness measurements for the fabrics were conducted as per the INDA standard test 90.1 (ASTM D5732) [29]. Fabrics were cut to $25.4 \times 2.54 \text{ cm}^2$ ($10 \times 1 \text{ inch}^2$) strips along the machine direction and two strips were measured for each fabric. The stiffness of each strip was measured on the face and back on both ends to get four readings for each strip. The results were averaged and the flexural rigidity/bending rigidity was calculated.

3.2.9 Tear strength

Tear strength was performed as per the INDA standard test 100.1 (ASTM D5734) [30] using Elmendorf trapezoid tear tester. Measurements were taken along the machine and cross directions. Fabrics were cut to $6.35 \times 7.65 \text{ cm}^2$ ($2.5 \times 3 \text{ inch}^2$) strips along both directions and an average of ten readings is reported. Test was carried out by attaching a single weight.

3.2.10 Fiber bundle orientation

Fiber bundle orientation was measured using WEBPROTM, an image analysis software [31]. Thirty images were captured along the machine direction and at 45° to the machine direction. The software analyzed the images and a fiber bundle distribution diagram was obtained.

3.2.11 Single bond test

Single bonds were tested by taking strips of fabric about 80mm*5mm. Cuts were made across the width of the strip in such a way that the two pieces are held together by a single bond point. The cuts were made very close to the periphery of the bond. A schematic of the test strip is shown in figure 3.2. This was tested on a United tensile tester with a gauge length of 2.54cm (1 inch) and a crosshead speed of 1.27cm/min (0.5 inch/min).

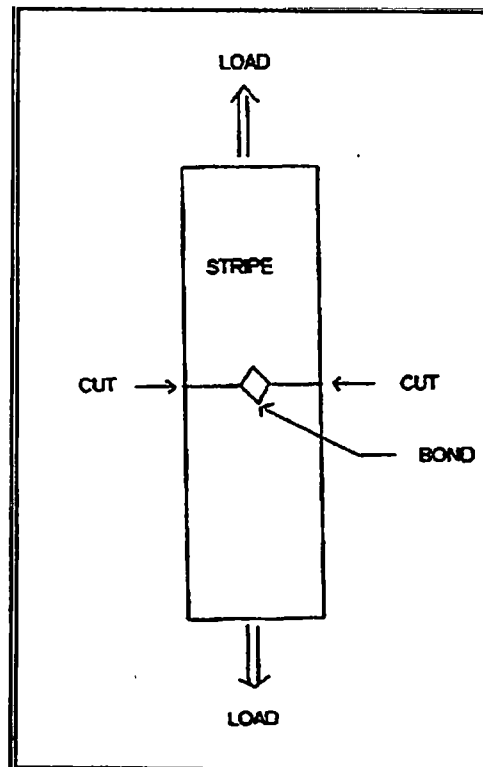


Figure 3.2. Schematic of the Single Bond Strip Test [8]

3.2.12 Scanning Electron Microscopy

Samples from fabric tensile testing were used to study the effect of increasing stress on the bond points and the fibers bridging the bonds. The Hitachi S-800 SEM was used to obtain the images of the ruptured specimens of fabrics. Successive images were obtained from the point where the fabric was clamped between the jaws in the tensile tester, towards the point where rupture occurred. To eliminate the effect of jaw break, only those samples, where the rupture area was not very close to the jaws were used for SEM.

Polypropylenes being a non-conducting polymer, samples were coated, and also the instrument was operated at very low voltage to minimize the charging. The accelerating voltage was kept constant at 1.5keV for all the samples. Back-scattered electrons were collected by the backscatter detector in topographic mode and analyzed. SEM pictures were obtained using a Polaroid camera.

CHAPTER IV

RESULTS AND DISCUSSION

4.1 Filament Properties

The filaments collected from the belt before bonding at all throughputs were tested for various thermal and tensile properties.

The properties of the unbonded filaments are shown in table 4.1. Filament diameter at all throughput rates was kept close to 18 micrometers by appropriately adjusting cooling and suction air speeds. The filament diameter values measured by image analysis technique (WebProTM) correlated well to those measured by optical microscopy technique. Although the actual values obtained from WebProTM were slightly higher than that obtained by direct measurement using microscope, the trends were same in both the cases.

The increase in air speeds with increase in throughput rates leads to higher level of drawing of the filaments and better packing of molecular chains in the filaments draw direction. This can be observed from the increased values of crystallinity and birefringence of the filaments with increase in throughput rate. The crystallinity values were calculated from DSC scans (figure 4.1). The DSC scans indicated that the peak melting temperature for all the filament samples was about 148°C.

Table 4.1. Filament Structural Features.

Throughput (ghm)	Basis weight (g/m ²)	Group code	Filament diameter (μm) Microscopy WebPro™		Birefringence	Crystallinity (%)
0.43	35	A	17.3	18.2	0.0205	35.6
0.35	20	B	-	18.1	-	-
0.35	35	C	18.0	18.5	0.0185	34.1
0.24	20	D	16.5	17.7	0.0167	33.3
0.24	35	E	-	18.4	-	-

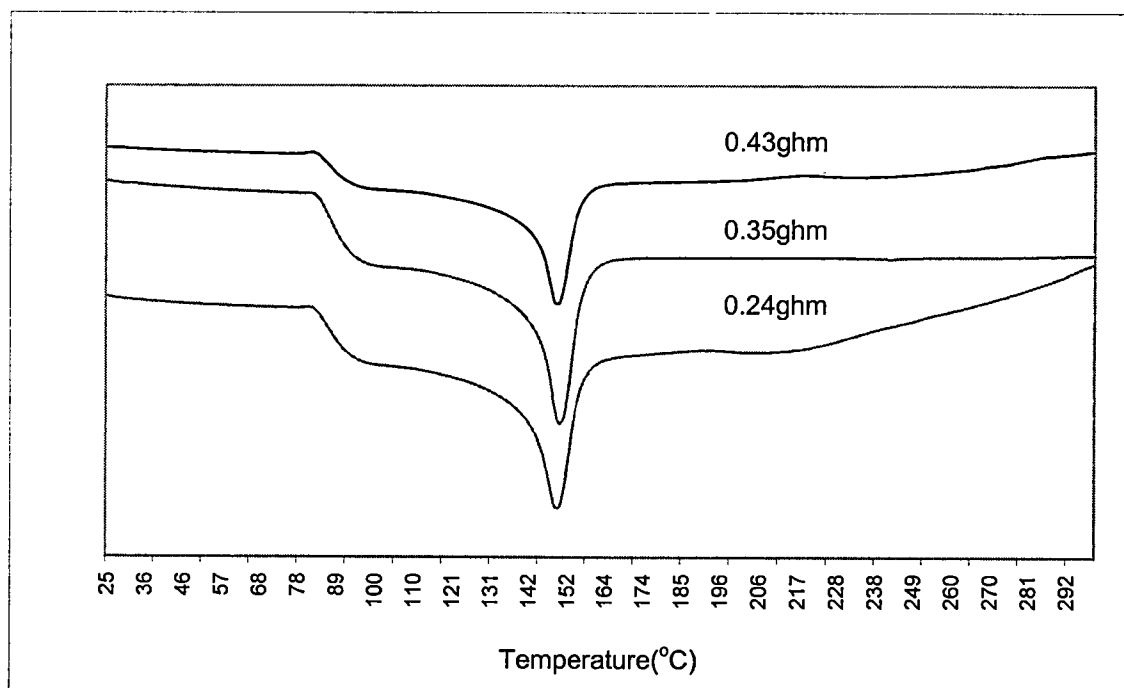


Figure 4.1. DSC Scans of Unbonded Filaments at different throughput rates.

Increase in crystallinity and crystalline orientation with increasing throughput was also observed from the x-ray data. This can be explained by the increasing intensity of the arcs and shortening of the arc lengths. The diffraction patterns obtained from the flat plate X-ray diffractometer are shown in figure 4.2.

Better packing and increase in orientation help in crystal growth. The wide-angle X-ray scans of filaments at different throughputs are shown in figure 4.3. For fibers produced at 0.24 and 0.35ghm throughput, the intensity vs 2θ scans are broad with no distinct peaks indicating a smectic structure. In the case of filaments produced at high throughput, the peaks are relatively narrow and sharp compared to the peaks at lower throughputs. This indicates a better development of filament morphology in case of filaments at high throughput rates. This is consistent with other data such as birefringence and is due to the higher draw achieved by increased air supply to achieve the same filament diameter.

The TMA scans of the filaments at different throughputs are shown in figure 4.4. The filaments produced at high throughput rate were thermally more stable compared to the filaments at lower throughput rates. This can be attributed to increased crystallinity, and thus a better developed morphology with increase in throughput rate.

The tensile properties of the mPP filaments are shown in table 4.2. The filaments show an increase in peak strength and decrease in peak elongation with an increase in throughput rate. This can be attributed to the higher orientation, and high crystallinity with increase in throughput, and is consistent with the structural features that were observed.

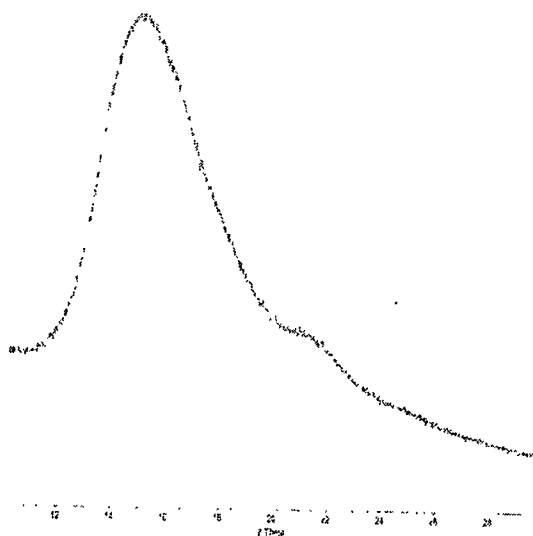


a. Filaments at 0.24ghm

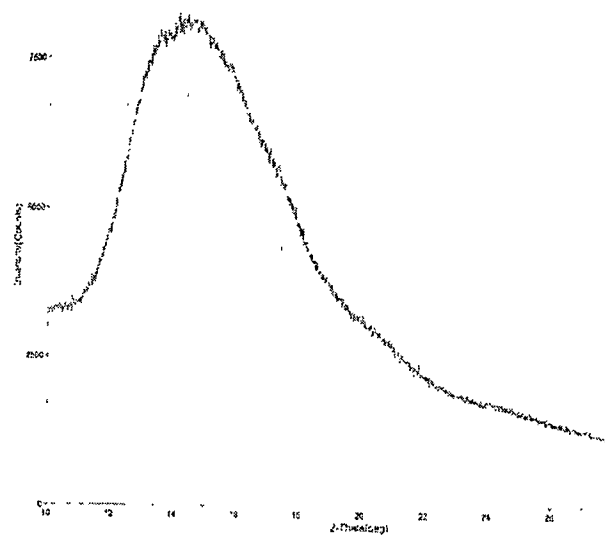


b. Filaments at 0.43ghm

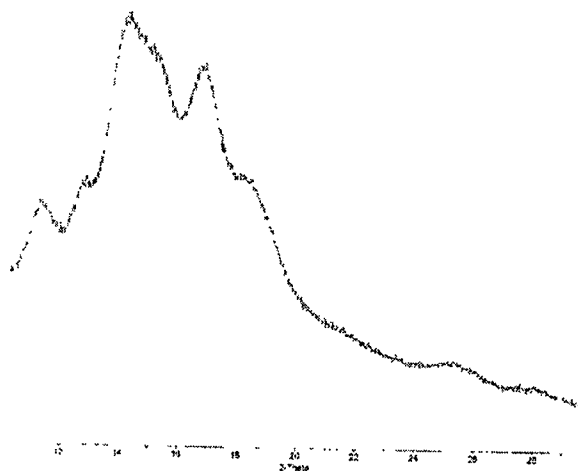
Figure 4.2. X-ray Diffraction patterns of filaments produced at different throughputs.



Filaments at 0.24ghm (4D)



Filaments at 0.35ghm (4C)



Filaments at 0.43ghm (4A)

Figure 4.3. WAXD Scans of the Filaments at different Throughput rates.

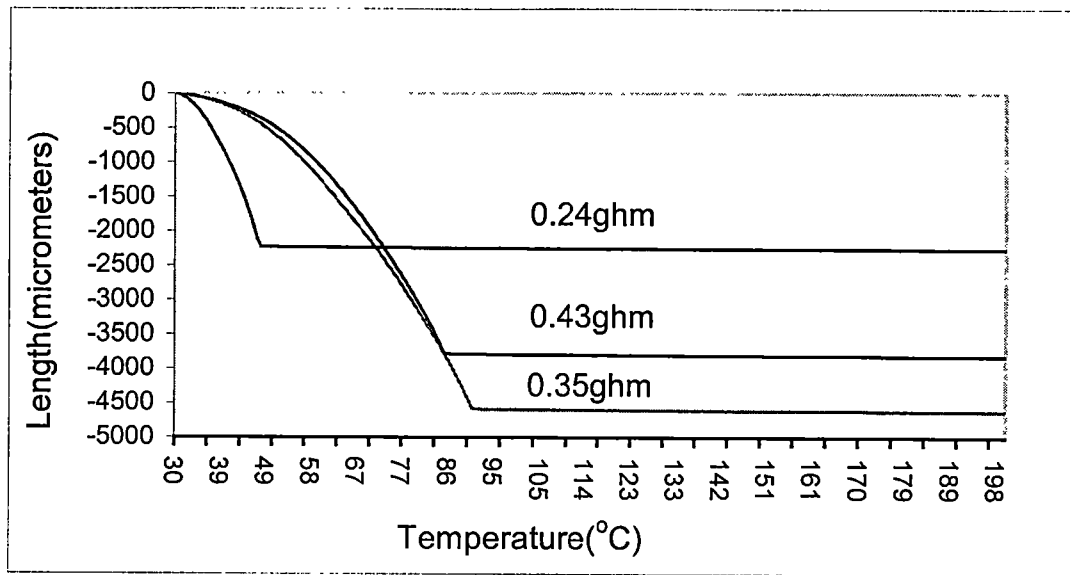


Figure 4.4. TMA Scans of Unbonded filaments at different throughputs.

Table 4.2. Filaments Tensile Properties.

Throughput ghm	Peak stress g/Tex	Peak extension %
0.24	34.6	162
0.35	45.3	133
0.43	67.3	120

4.2 Comparison of the polymer and filament properties of znPP and mPP

4.2.1 Polymer Viscosity

The figure 4.5 shows the comparison of the shear viscosity of the znPP and mPP resins over a shear rate range of 10 to 1000 sec^{-1} at 230°C. The znPP resin has a MFR of 35 while the mPP resin was of 32 MFR. The metallocene resin has shown higher viscosity than znPP resin over the entire shear rate region. This behavior of mPP resins is different from the one reported in earlier studies [3]. This may be due to differences in MWD of the grades.

4.2.2 Fiber Structure

The DSC scans of the mPP and znPP filaments at 0.43ghm throughput rates are shown in figure 4.6. The melting point and crystallinity of mPP filaments were lower than that of znPP filaments. The melting temperature shows a difference of approximately 12-13°C between them. ZnPP has a crystallinity of 43.9% and a peak melting temperature of 162°C, while mPP showed a crystallinity of 35.6% and a peak melting temperature of 148°C. Similar differences were observed at other throughputs as well (See Appendix 1). Bond *et al*, [23] explained the reason for this as metallocene catalyzed resins crystallize more slowly than the Ziegler-Natta catalyzed resins at a given temperature. The melting temperature data indicated that the crystalline lamellae produced by the metallocene resin are not as stable as the lamellae produced by the Ziegler-Natta resins, thus they melt at lower temperatures. In fact the differences in crystalline structure of mPP compared to that of znPP [8] is clear from WAXD data as well as birefringence values. Both crystallinity and orientation of mPP are less than that

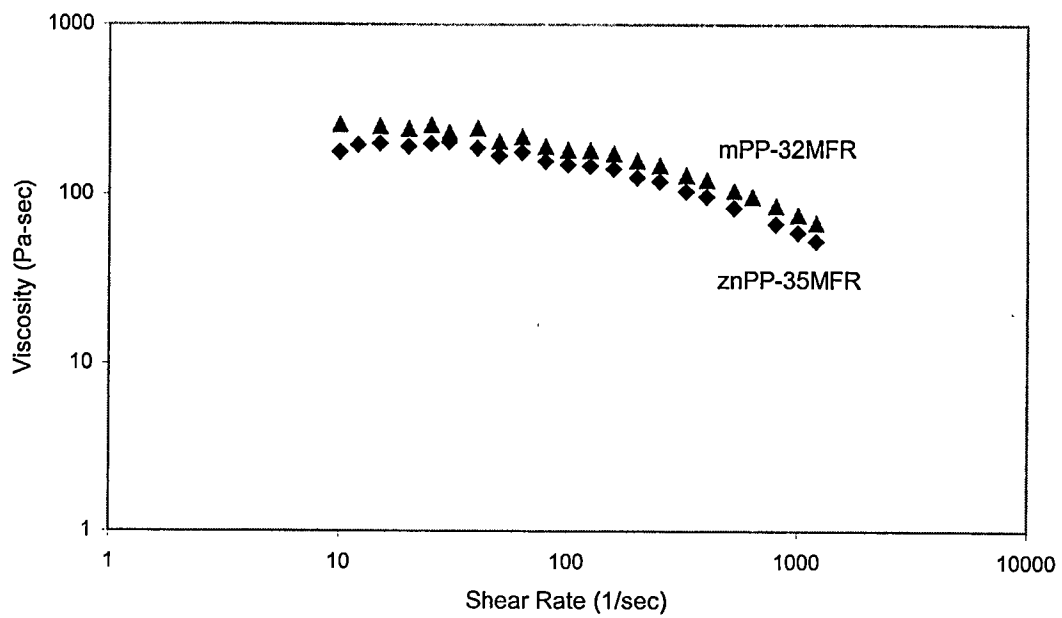


Figure 4.5. Shear Viscosity of znPP and mPP polymers.

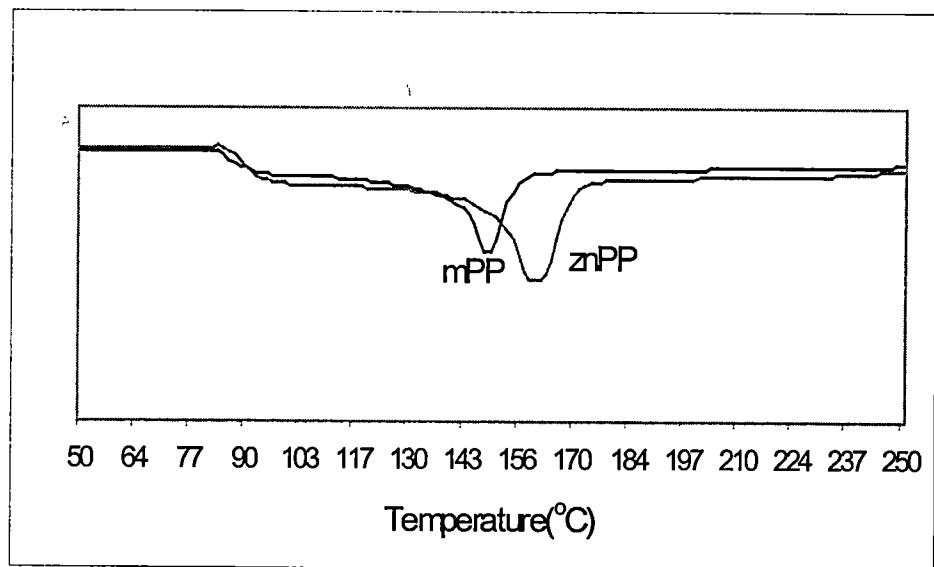


Figure 4.6. DSC Scans of the filaments produced at 0.43 ghm.

of znPP under similar processing conditions. The crystallinity of the mPP filaments was lower than the znPP filaments. This may be due to occasional reversal of head-to-tail polymer chain growth that hinders crystalline growth as explained by Bond *et al.* [23].

4.2.3 Thermal Response

The TMA scans of znPP and mPP filaments are compared in figure 4.7. The filaments produced with mPP are thermally less stable compared to the filaments produced with znPP. This can be attributed mainly to the difference in the melting point of the filaments. In addition to the differences in melting temperature, morphological differences such as lower crystallinity make mPP easily deformable under heat and stress. This is an indicator that mPP is easily bondable in thermal bonding.

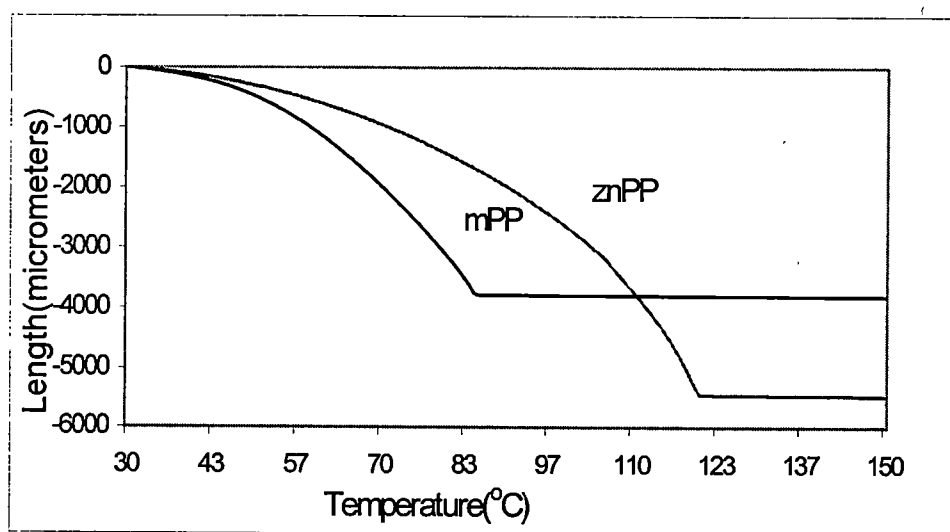


Figure 4.7. TMA Scans of the filaments produced at 0.43 ghm.

4.2.4 Tensile Properties

The tensile properties for the mPP and znPP filaments are shown in table 4.3. The mPP filaments have shown an increase in peak stress and a decrease in elongation with increase in throughput. This can be attributed to better orientation and well-developed filament morphology at higher throughputs. The filaments of mPP are stronger than the filaments of znPP. The strength values were nearly one and half times greater than that of znPP filaments. This difference may be due to the differences in polymer characteristics and their processing behavior. Achieving higher strengths with almost similar process conditions is one of the advantages of mPP polymers. However, the elongation percentage of metallocene filaments were nearly half of the znPP filaments.

Table 4.3. Comparison of Properties of the Filaments.

Throughput rate ghm	Peak Strength (g/Tex)		Peak Extension (%)		Crystallinity (%)		Birefringence	
	mPP	znPP	mPP	znPP	mPP	znPP	mPP	znPP
0.24	34.6	24.0	162	312	33.3	43.6	0.0167	0.0223
0.35	45.3	23.7	133	297	34.2	43.6	0.0185	0.0230
0.43	67.4	25.2	120	296	35.6	43.9	0.0205	0.0220

4.3 Fabric Properties

Spunbonding process is a continuous one and hence changing one process condition necessitates changes in other process conditions. To produce a fabric of same basis weight at different throughput rates necessitates changes in the collector speed, which in turn affects the residence time of the web in the calender rollers. The bonding process is an inherent part of the spunbonding process and is also affected by the various spinning conditions. The choice of bonding conditions will have to take several of these factors into consideration to produce a fabric with optimum properties. The effect of some of the process conditions on the fabric properties is discussed in the following sections. The tensile properties of the fabrics along the machine direction and the cross direction are included in Appendix 2.

4.3.1 Effect of throughput rate

The effect of increasing throughput at constant fabric weights on tensile strengths of fabrics bonded at 110°C is shown in figure 4.8. At constant fabric weight, with an increase in throughput there is a decrease in peak stress. This is due to the lower residence time between calendar rollers and due to difference in filament morphology. As explained earlier, filaments at higher throughputs have better developed morphology and so require relatively high bonding temperatures to form an optimum bond. The TMA scans of the filaments had clearly shown that fibers produced at higher throughputs were thermally more stable requiring higher temperature to deform. The low strengths at higher throughputs is due to insufficient bonding and this is explained later from SEM pictures of bond areas.

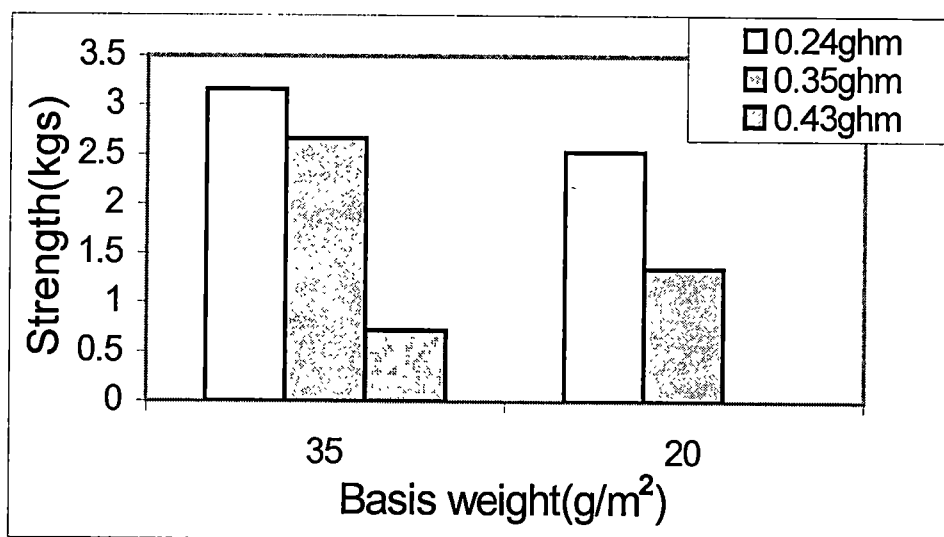


Figure 4.8. Peak Strength in MD with increasing throughput and 110°C bonding temperature.

The effect of throughput at 140°C is shown in figure 4.9. Even at 140°C, with high fabric weights, a slight decrease in strength with increase in throughput rate is observed. But at higher bonding temperatures the values of strength are more than double in case of high basis weight fabrics. This is due to better bonding of the filaments at higher temperatures in case of high fabric weights. At lower basis weights, we observe an increase in strength with an increase in throughput rate even though there is a decrease in the residence time. This may be due to the high bonding temperature that might have lead to better bonding of the filaments. In case of fabrics produced at low throughput rate there is a decrease in strength value at low basis weights from 110°C to 140°C. This may be due overbonding at higher temperatures for this group of fabrics.

Tear strength of the fabrics also decreases with an increase in throughput rate at lower bonding temperature of 120°C and is shown in figure 4.10. At a high temperature of 140°C (figure 4.11) there is an increase in tear strength of the fabrics, which can be attributed to better bonding and better filament properties. The fabrics produced from both the polymers i.e., znPP and mPP have shown similar trends in the throughput effect. The bending rigidity of the fabrics increased with an increase in throughput at lower bonding temperature of 120°C and this is shown in figure 4.12. This trend is probably due to differences in fiber morphology and tensile properties.

4.3.2 Effect of Fabric weight

The effect of increasing fabric weights at constant throughput rates leads to reduced speed of collector. This increases the residence time of webs with high fabric

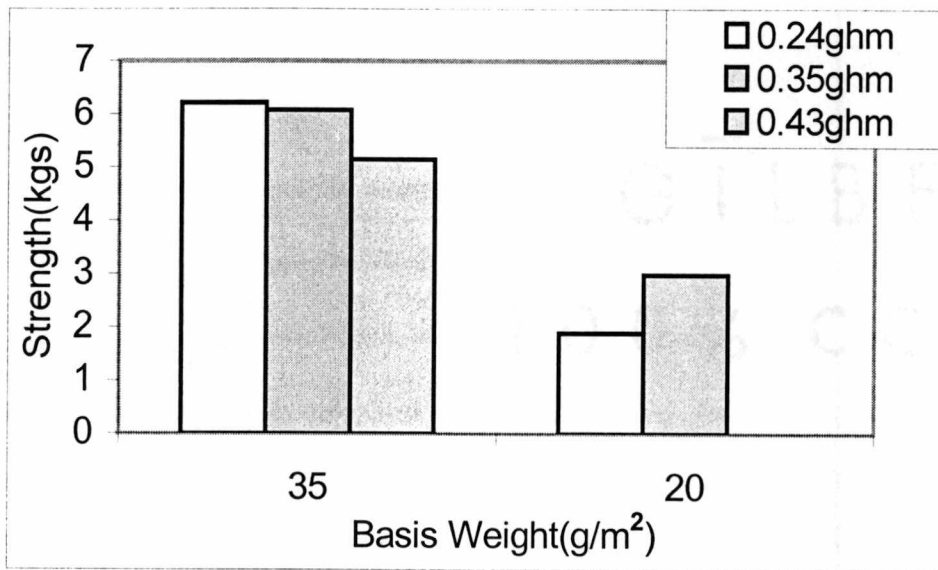


Figure 4.9. Peak Strength in MD with an increasing throughput and 140°C bonding temperature.

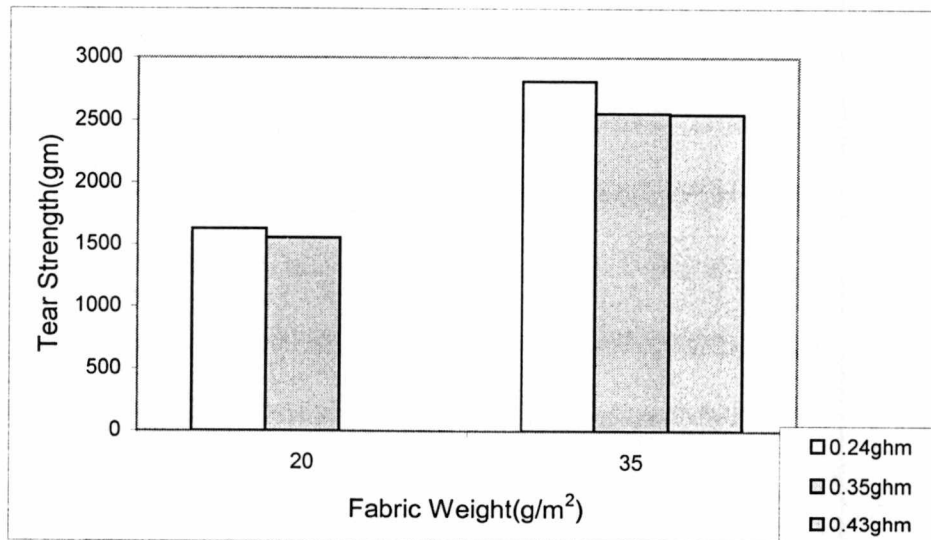


Figure 4.10. Tear Strength in MD with an increasing throughput and 120°C bonding temperature.

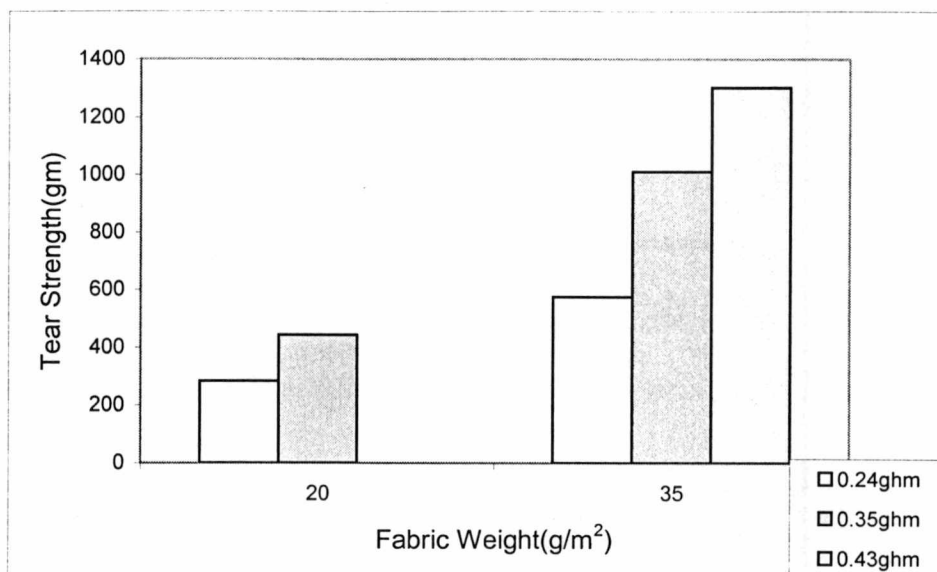


Figure 4.11. Tear Strength in MD with an increasing throughput and 140°C bonding temperature.

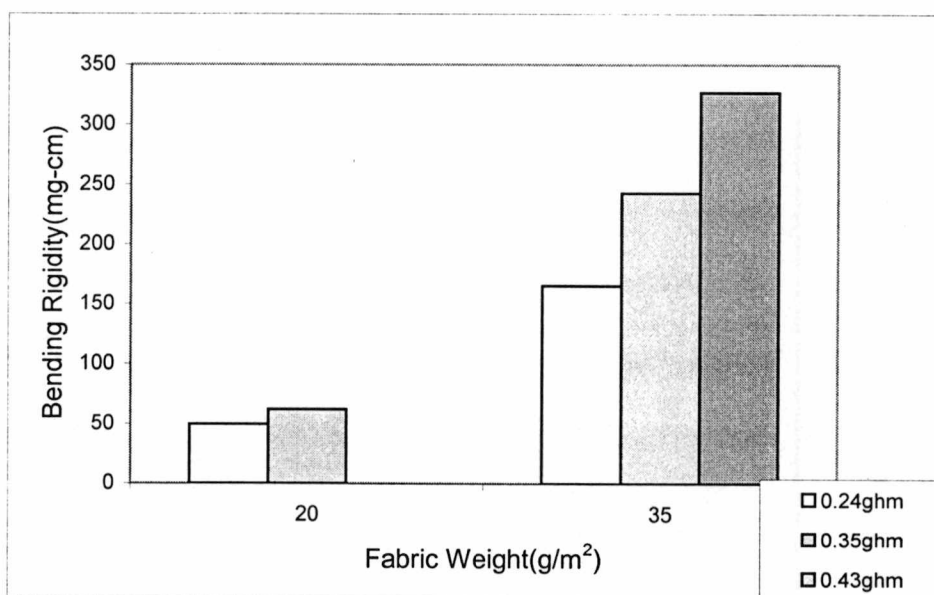


Figure 4.12. Bending Rigidity in MD with increase in throughput and 120°C bonding temperature.

weights for the same throughput. The effect of increasing basis weight on fabric strengths at constant throughput rate and at temperatures of 120°C and 140°C are shown in figures 4.13 and 4.14 respectively. At lower bonding temperature, the strength value at high throughput is less than that at low throughput. This may be due to decrease in contact time and the difficulty to transfer heat to the center of the web at low bonding temperatures.

High bonding temperatures with high nip pressures are required for bonding of heavier fabrics. At high bond temperatures of 140°C, higher strengths of fabrics at high throughput rates were observed. High temperatures help in efficient heat transfer through the thickness of the web. Obviously, higher bonding temperatures are required for high basis weights to achieve optimum strength, in spite of increase in residence time due to lower belt speed. In fact, the residence time is almost twice for 0.43 throughput compared to that at 0.24 throughput for the same fabric weight. One more important observation was that actual strength values were higher for samples bonded at 140°C (~ 6kg) compared to that bonded at 120°C (~ 3kg) for both fabric weights. Similar trends were observed in the cross direction as well, although the actual values were about half of that observed for machine direction.

As expected, the tear strength increases with increase in basis weight. This is consistent across all the throughputs and bonding temperatures as shown in figures 4.15 and 4.16. This is due to increase in number of filaments participating in the tearing process at higher basis weights. Also, with an increase in bonding temperature, the tear strength values decreased due to improved bonding which is consistent with earlier observations [8].

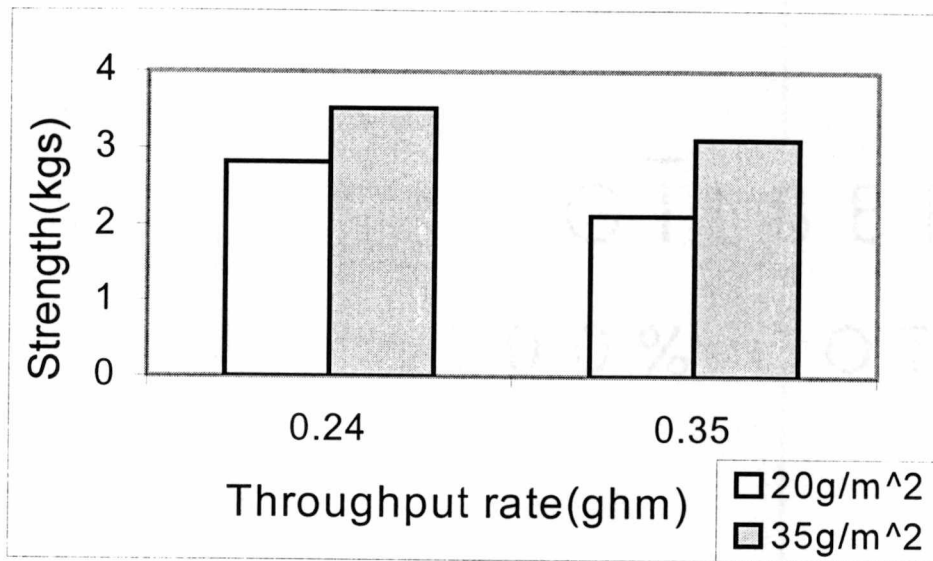


Figure 4.13. Peak Strength with increasing Fabric weights and 120°C bonding temperature.

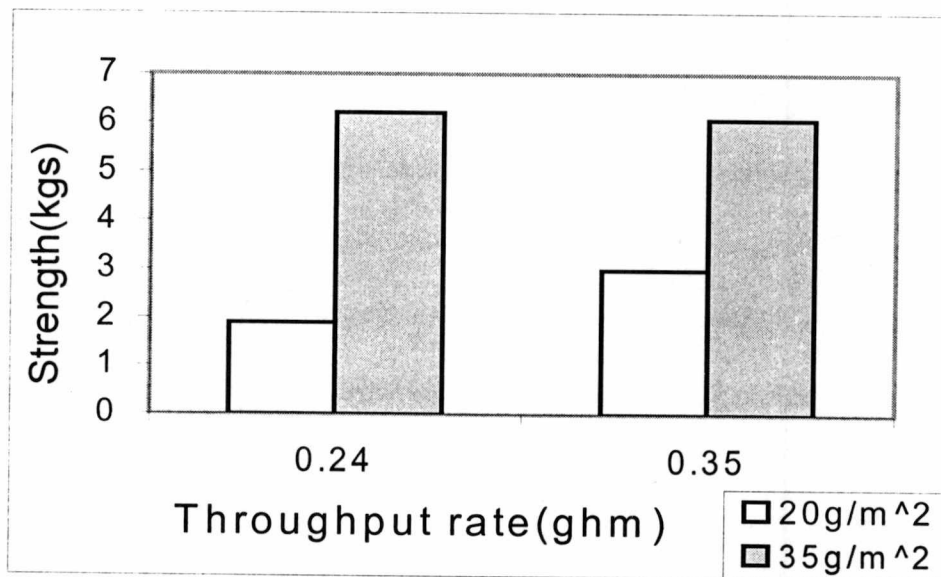


Figure 4.14. Peak Strength with increasing Fabric weights and 140°C bonding temperature.

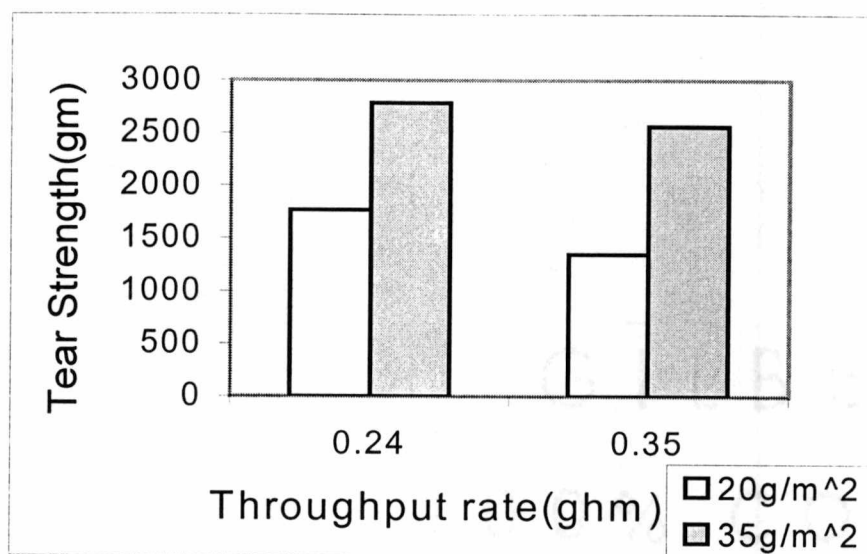


Figure 4.15. Tear Strength in MD with increasing Fabric weights and 110°C bonding temperature.

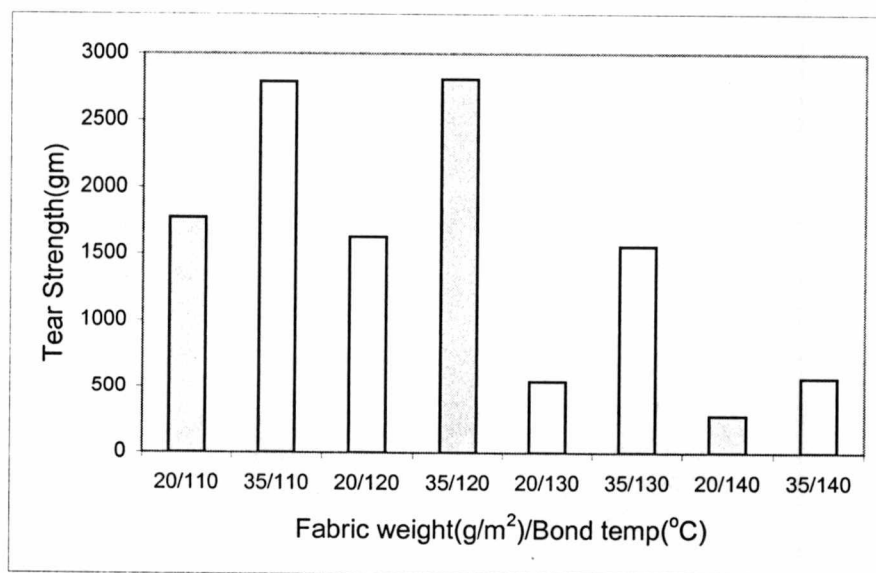


Figure 4.16. Tear Strength in MD with increasing Fabric weights and bonding temperatures at 0.24 throughput.

The stiffness of the fabrics increases with basis weight and bonding temperatures at all throughputs as shown in figure 4.17. This is an expected trend due to increasing material weight and improved bonding.

4.3.3 Effect of Bonding Conditions

The bonding conditions varied during processing were calender temperature, residence time and calender nip pressure. The effects of residence time have already been discussed. Nip pressure was increased for higher basis weights as recommended by the machine manufacturer. By properly selecting the bonding temperatures we can compensate for the changes in the line speed due to changes in

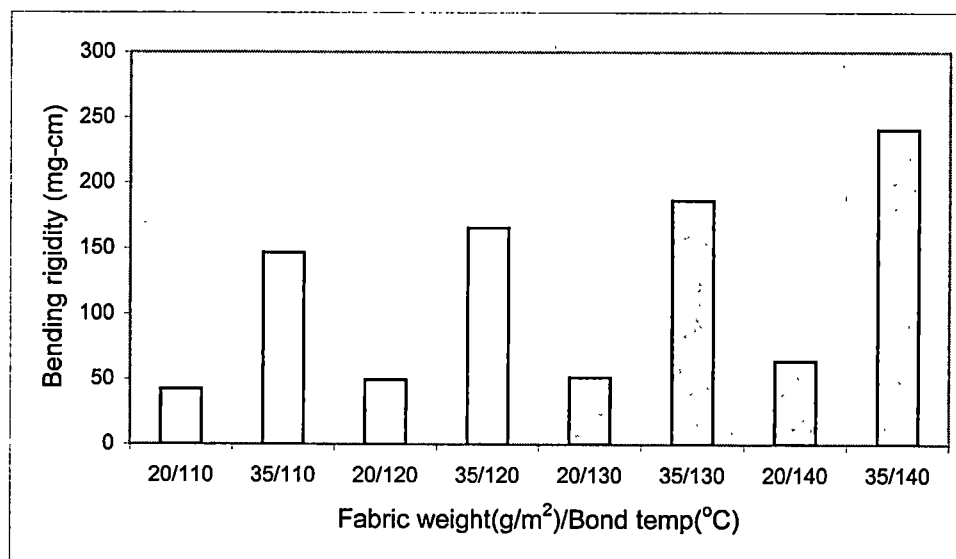


Figure 4.17. Bending Rigidity in MD with increasing fabric weight and bonding temperatures at 0.24 throughput.

throughput or basis weights. As shown in figure 4.18, with an increase in bonding temperature, all groups of fabrics except that produced at 0.24ghm and 20gsm fabric weight (group D), have shown an increase in peak stress values. The elongations of the fabrics as shown in figure 4.19, has shown an initial increase and then decrease in the case of fabrics of low weight. For higher weight fabrics, we see an increase in elongation values with an increase in bonding temperature. In all these cases, it is possible that the optimum conditions have not been achieved. In group D, it is observed that with increase in temperature the peak stress increases, reaches maximum and then decreases. Similar trends are observed even in cross direction (See Appendix-2). The bonding temperature at which certain sample exhibits optimum strength depends on throughput rate, basis weight, residence time and bonding temperature. Earlier studies with znPP have shown that for almost all groups of fabrics, with an increase in bonding temperature strength values increased and then the values dropped beyond the optimum temperature. The optimum bonding temperature varied with filament morphology and line speed. Optimum bonding temperature is less than 140°C in the case of group D, where as for other samples, optimum temperature is 140°C or higher than that, since in the range of conditions investigated only an increasing trend in strength and elongation has been observed. As seen from figure 4.20, there is a reduction in tear strength of fabrics produced at low throughput rates with an increase in temperature. This may be due to the embrittlement of the bond sites and loss of fiber structure in the bond areas. This inhibits the movement of the filaments, and prevents bunching together of the filaments against tearing. At higher throughputs, initially there is an increase in tear strength and then

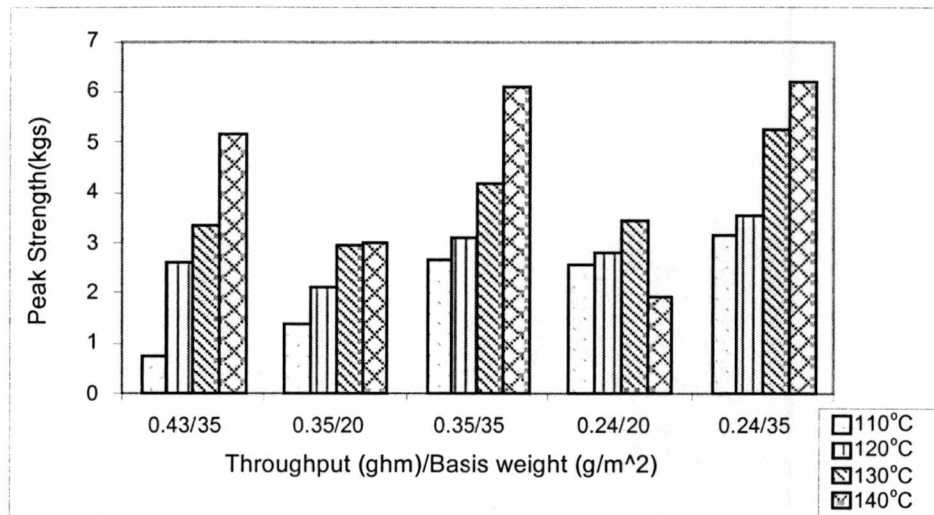


Figure 4.18. Peak Strength in MD with increasing bonding temperatures.

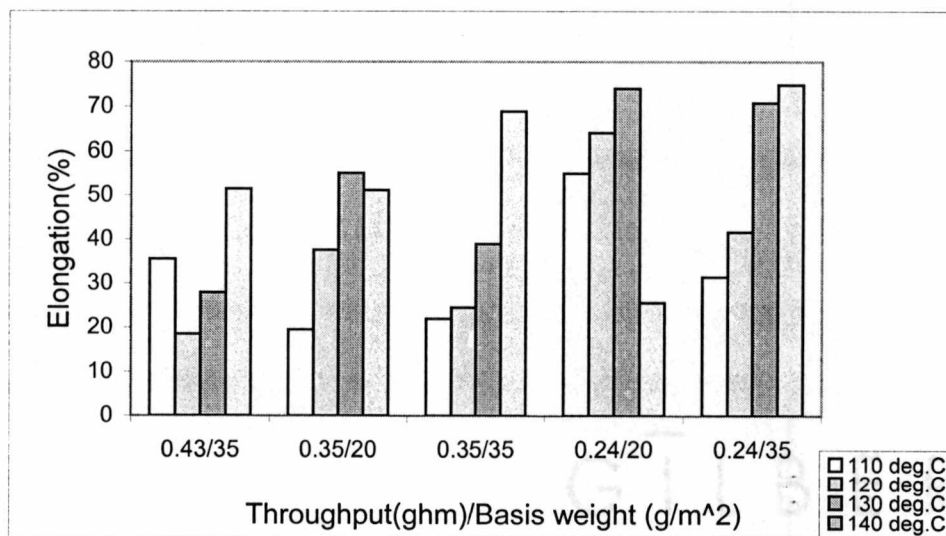


Figure 4.19. Peak Elongation in MD with increasing bonding temperatures.

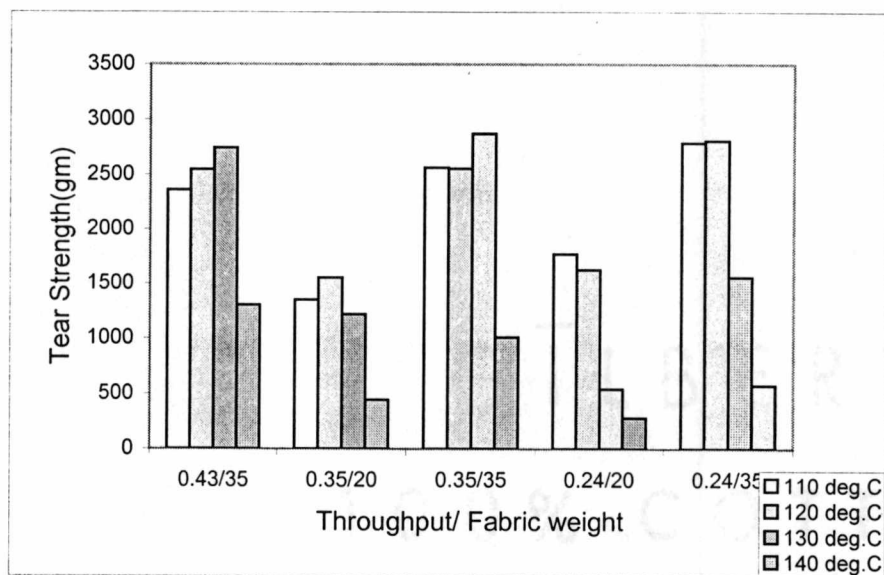


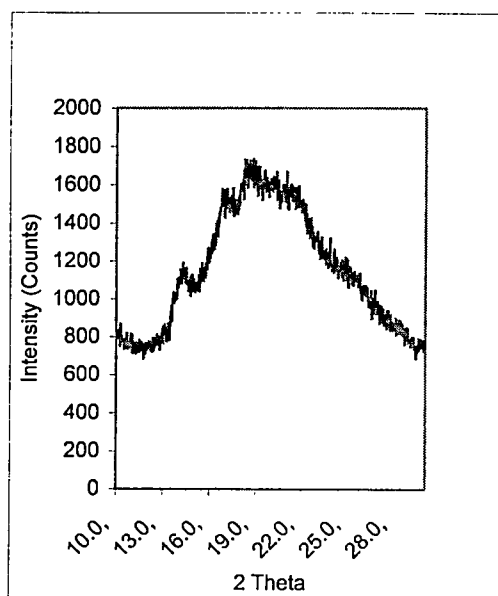
Figure 4.20. Tear Strength in MD with increasing bonding temperatures.

decrease. This may be due to better structural properties of filaments, which make them loose their structure at high temperatures. From this figure, we can say that optimum tear strength value moves towards higher temperature with an increase in throughput rate or fabric weights. If one considers tear strength values, it appears that optimum bonding temperatures in the range of 130°C for higher throughputs of 0.35 and 0.43ghm and about 120°C for a lower throughput of 0.24ghm. The trends observed in tensile strength and elongation of the fabrics in the cross direction are similar to the trends in the machine direction (See Appendix 2).

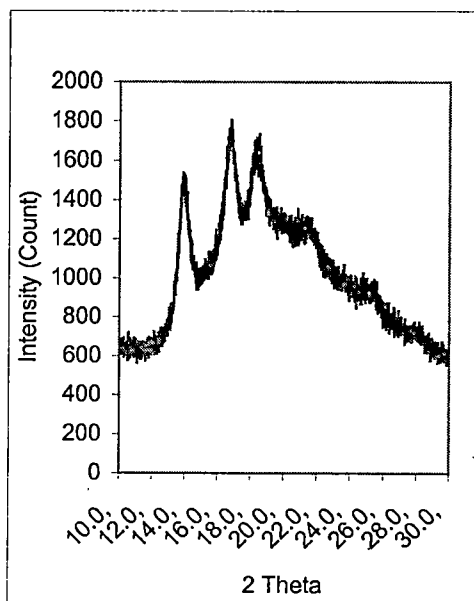
The process of thermal bonding can be viewed as an annealing process and hence changes in the morphology of the filaments would be expected as a consequence of bonding. For the fabrics produced at constant throughput and basis weights, with an increase in bonding temperature there is an increase in the size of the crystallites in both bonded and unbonded regions of the fabrics. This can be observed from the wide-angle x-ray scans shown in figure 4.21. Increasing size of the crystallites, characterized by sharper peaks can also be seen from figure 4.22, as we go from the unbonded filaments to the bonded area. More intense peaks were observed in bonded areas than in the unbonded areas. These trends of change in filament morphology from the unbonded region to bonded region were also observed in the case of fabrics produced with Ziegler-Natta catalyzed polypropylene fabrics.

4.3.4 Rupture mechanism

For better understanding of the failure mechanism of these fabrics, the bond points of the fabrics subjected to tensile stress were observed under SEM. This also

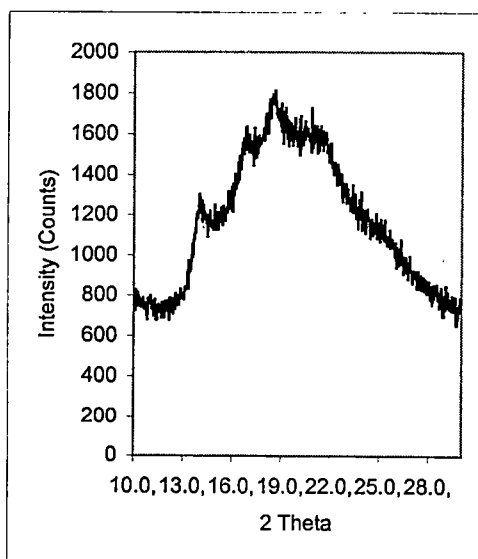


110°C

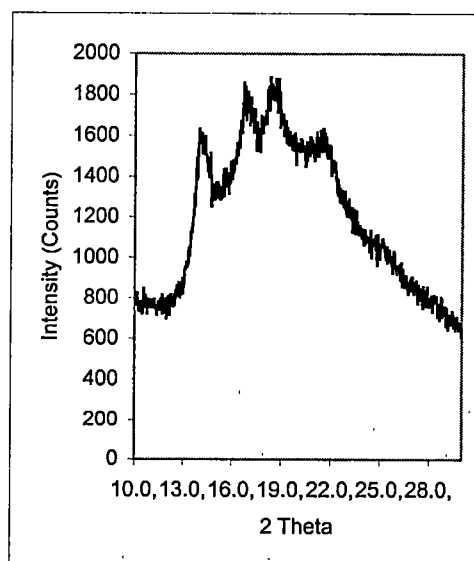


140°C

Bonded regions



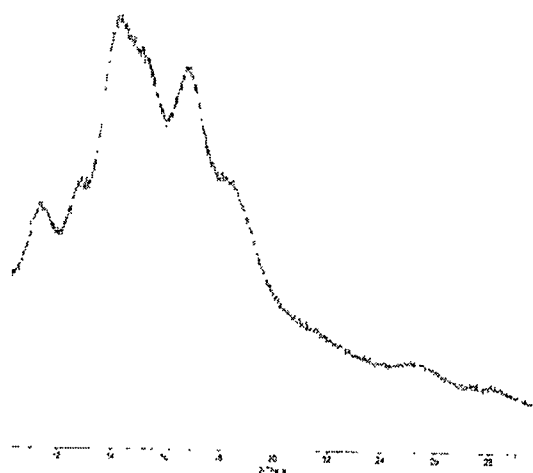
110°C



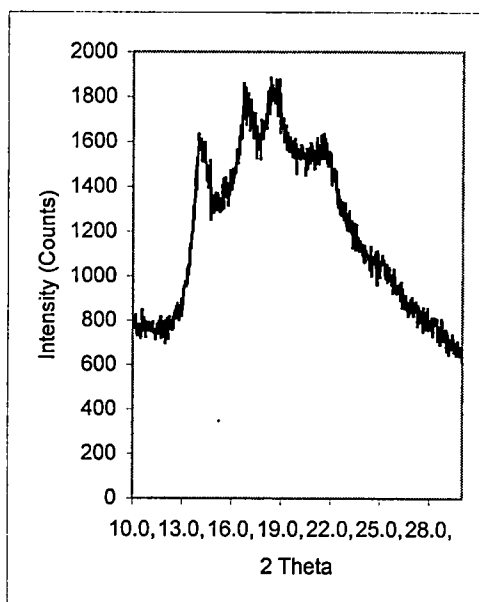
140°C

Unbonded regions.

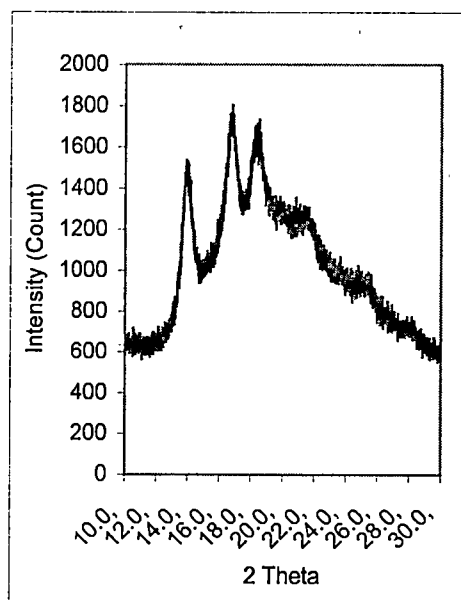
Figure 4.21. WAXD scans of the filaments.



a



b



c

Figure 4.22. WAXD Scans of Filaments Produced at 0.43ghm/35g/m²/140°C.

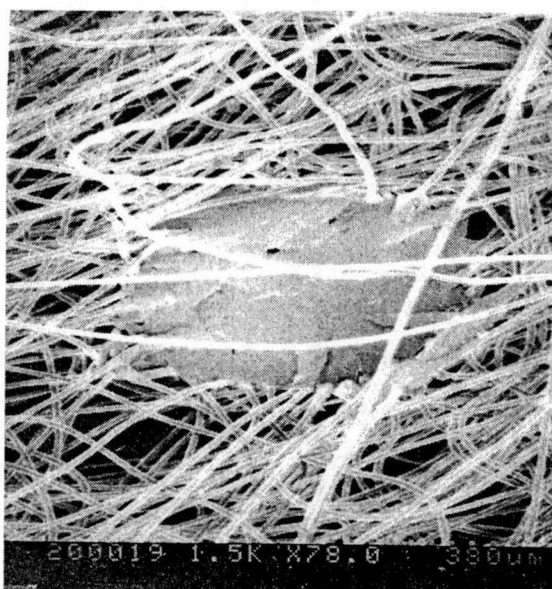
a. Spun Filaments b. Unbonded Area c. Bonded Area

provides vital information about the structure of the bond. As shown in figure 4.23, with an increase in bonding temperature, at constant throughput of 0.24ghm and fabric weight of 20g/m^2 , a better bond structure has been observed. The filaments at higher temperature lose their individual identity and form a better bond. There seems to be a good partial melting of fiber surfaces and flow of polymer between adjacent fibers resulting in efficient inter filament bonding. These different bond structures have important consequences on the properties and the rupture mechanism. The fabrics subjected to tensile test, after the completion of the test were observed at different positions to study the behavior of the bond points. Earlier studies had shown that the stress concentration increases as we go from the point of clamping of the specimen towards the center, where the rupture usually occurs [32]. The effects of shear stress due to the 'necking' of the specimen at the corners have been minimized by observing the bond points at the center along the width of the fabric.

The figures 4.23, 4.24 and 4.25 show SEM pictures of group D ($0.24\text{ghm}-20\text{g/m}^2$) fabrics that have shown a trend of increase in stress with increase in temperatures and later decrease at high temperatures. From the pictures in group-a, it is clear that a well formed bond point is observed with the increase in temperatures. As the stress level increases (figure 4.24), at lower bonding temperatures, one can see the filaments coming out of the bond (dissociation of the bond) and also the stretching of the bond. Finally at high stress levels (figure 4.25) complete dissociation of the bond is observed for samples bonded at a lower temperature. For fabrics bonded at a high temperature of 140°C any dissociation of the bond as seen at 130°C and lower temperatures is not observed. But,



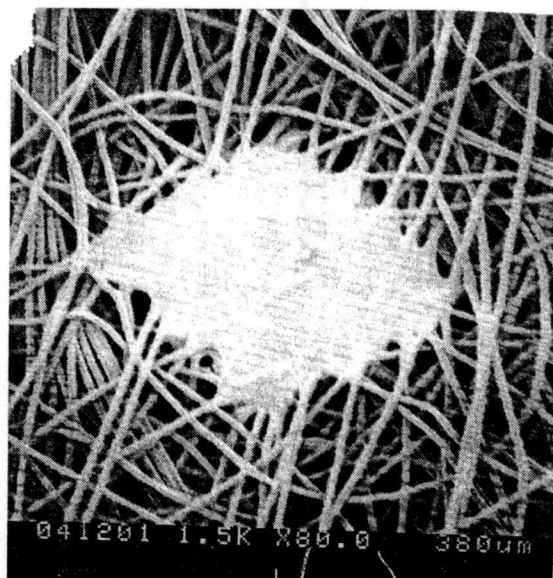
110°C



120°C



130°C



140°C

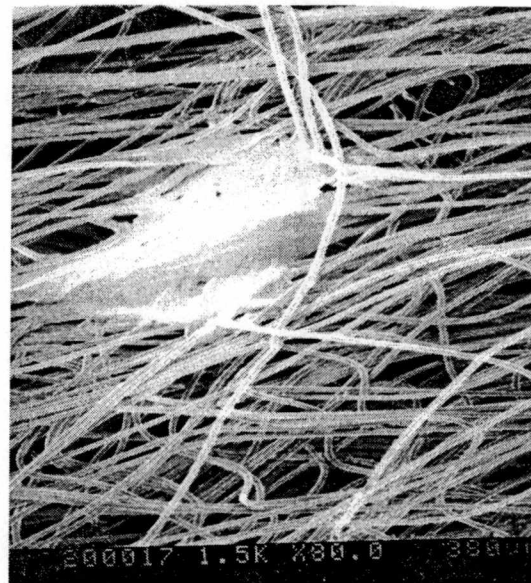
Group a

Figure 4.23. SEM pictures at 0.24ghm throughput, 20g/m² basis weight

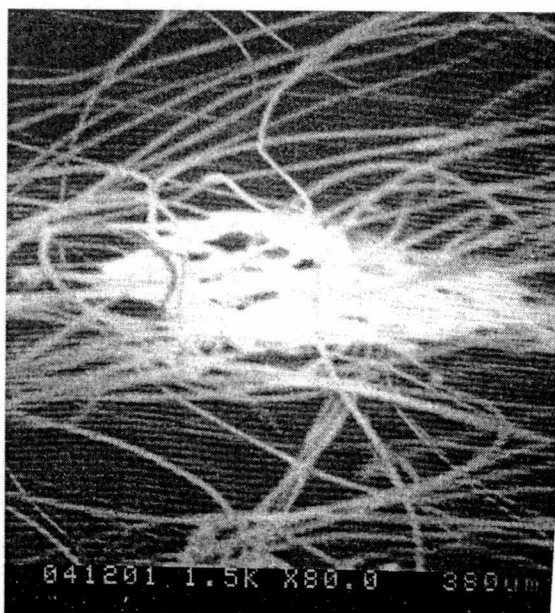
(Groups a-c denotes pictures taken at increasing stress levels)



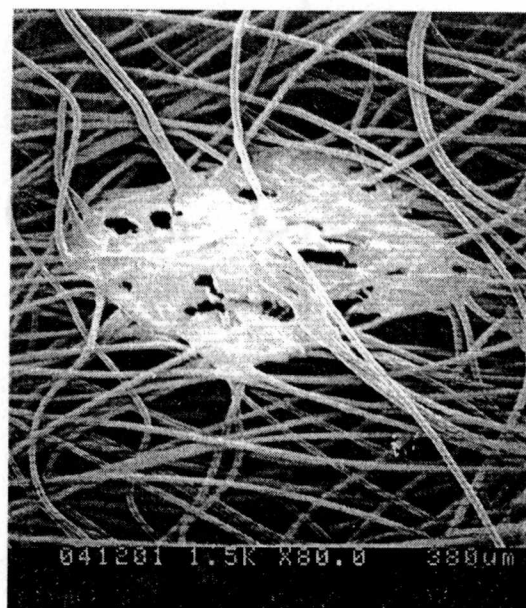
110°C



120°C



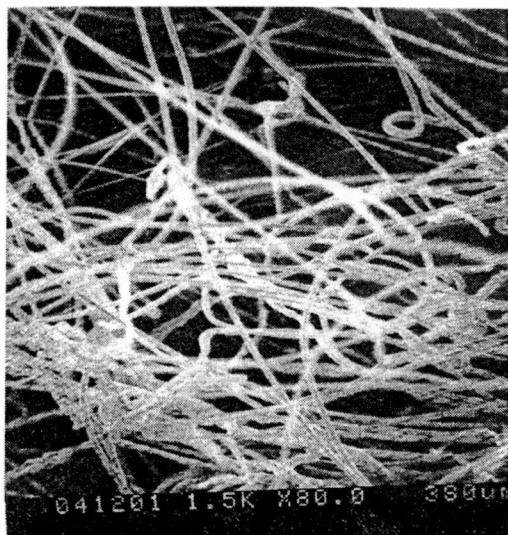
130°C



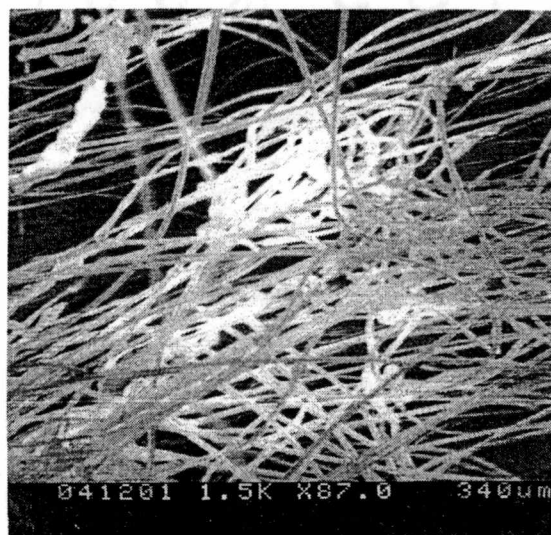
140°C

Group-b

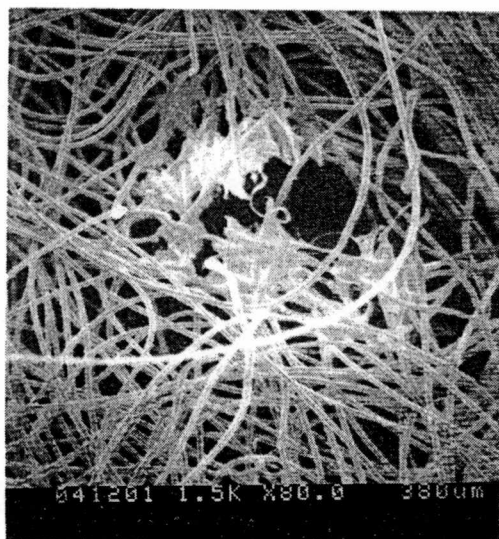
Figure 4.24. SEM pictures at 0.24ghm throughput, 20g/m² basis weight



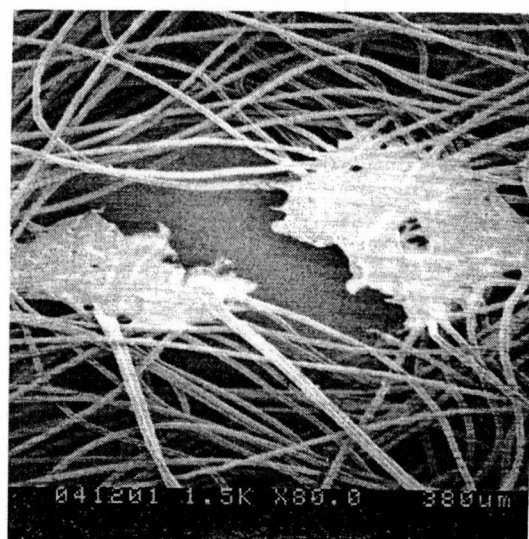
110°C



120°C



130°C



140°C

Group-c

Figure 4.25. SEM pictures at 0.24ghm throughput, 20g/m² basis weight

there are lot of holes in the bond area and finally the complete breakage of the bond occurs. This may be due to overbonding of the filaments. This group of fabrics has shown optimum strength at 130°C. Such a failure mechanism may be due to the initial disassociation and final breakage of the bond points observed in this group of fabrics. For other groups of fabrics, there is no evidence of the breakage of the bond even at higher temperature. It is apparent that overbonding conditions for these groups have not been reached and thus there is an increase in strength even at 140°C. This coincides with the tensile test values observed for these groups.

4.3.5 Single Bond Test

The single bond strengths of all groups of fabrics are shown in table 4.4. Testing of a single bond as described earlier agrees with the trends observed with the fabric strengths in most of the cases. In the case of single bond strengths, with increase in throughput, keeping basis weight and bonding temperature constant, a decrease in strength values (look at the values of 1E, 1C and 1A) due to the reduced residence time in the nip of the calender was observed. Coming to the basis weight effect, higher the basis weight higher the strength mainly due to more number of filaments participating in the bond.

Looking at the bonding temperature, at constant basis weight and throughput rate with increase in temperature an increase in strengths has been observed. In case of fabrics produced at low throughput and basis weights i.e., 0.24/20, as shown in figure 4.26, the shape of the load elongation curve is different. Initially at lower bonding temperatures the strength is low and at higher temperatures, the load is higher.

Table 4.4. Single bond strengths of various groups of fabrics.

Throughput/ fabric wt./ Bonding temperature	Peak Load (lbs)
0.43/35/110 (1A)	0.196
0.43/35/120 (2A)	0.299
0.43/35/130 (3A)	0.574
0.43/35/140 (4A)	0.581
0.35/20/110 (1B)	0.416
0.35/20/120 (2B)	0.403
0.35/20/130 (3B)	0.329
0.35/20/140 (4B)	0.317
0.35/35/110 (1C)	0.410
0.35/35/120 (2C)	0.457
0.35/35/130 (3C)	0.524
0.35/35/140 (4C)	0.752
0.24/20/110 (1D)	0.247
0.24/20/120 (2D)	0.193
0.24/20/130 (3D)	0.332
0.24/20/140 (4D)	0.330
0.24/35/110 (1E)	0.543
0.24/35/120 (2E)	0.543
0.24/35/130 (3E)	0.648
0.24/35/140 (4E)	0.764

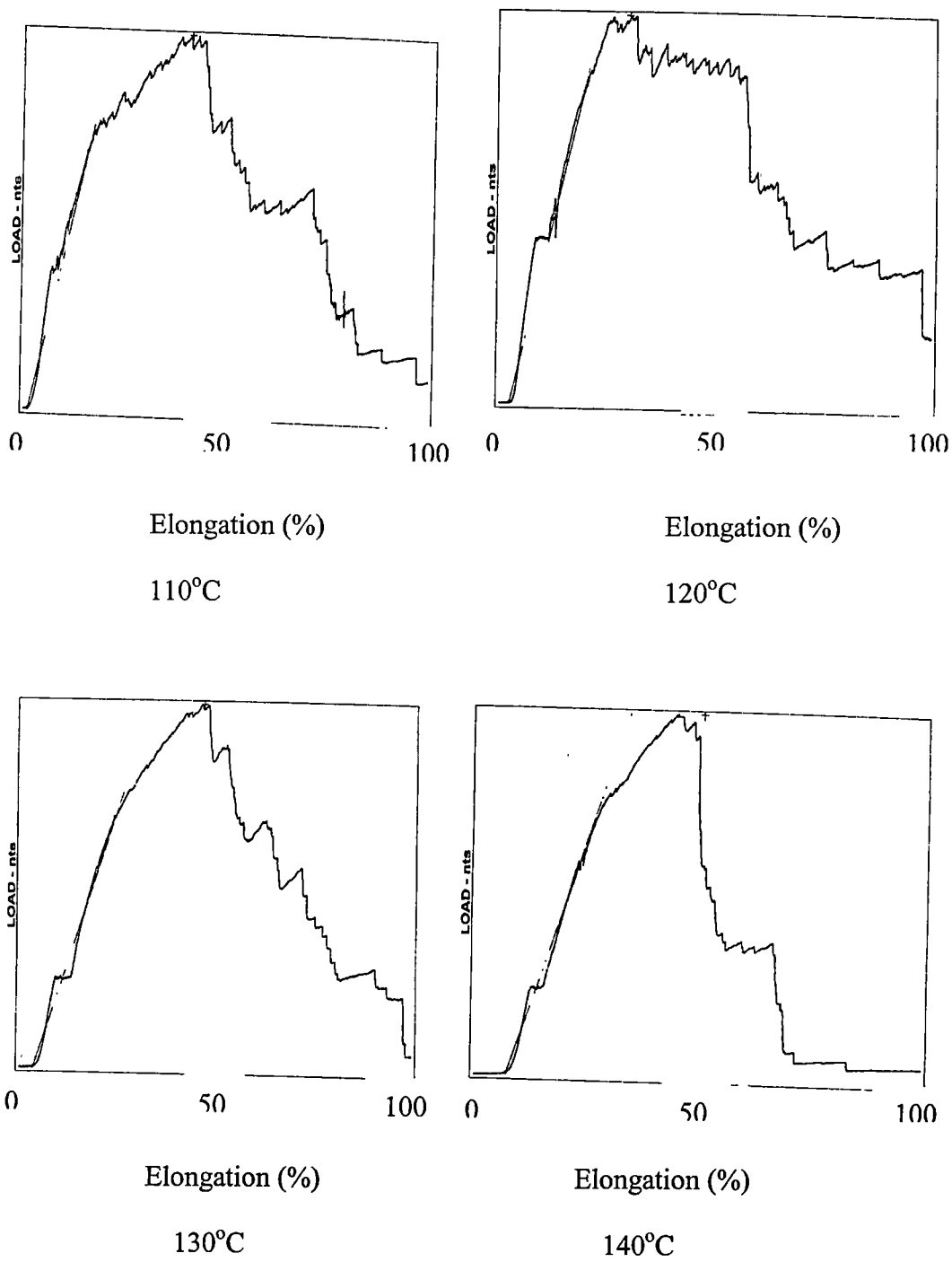


Figure 4.26. Load-Elongation curves at different temperatures of fabrics produced at 0.24ghm throughput and 20g/m² basis weight.

4.3.6 Comparison of Fabric Properties of mPP and znPP

The tensile properties of mPP fabrics were compared to strengths of znPP fabrics reported earlier [12]. The process conditions chosen were similar in both the cases. However, the design was restricted to two basis weights and the bonding temperatures chosen were less by nearly 10°C. The comparison has clearly shown that the fabrics produced with mPP have higher strength and elongation values than that produced with znPP almost at all process conditions. Figures 4.27 and 4.28 show the comparison of values of strength and elongation of the fabrics produced at 0.24 ghm throughput rate and 35g/m² basis weight in MD. Similar trends were also seen in CD (See Appendix 2).

The tear strength of mPP fabrics had shown similar trends to that of comparable znPP fabrics. The values of the strengths were almost equal at most of the process conditions.

Comparison is also made between the bending rigidity of both types of fabrics. The fabrics of mPP produced at throughput of 0.24ghm, 35g/m² fabric weight and bonding temperatures of 120 and 140°C have shown slightly higher bending rigidity values than comparable znPP fabrics. Similar trend was also observed even at higher throughput rates.

The mechanisms of rupture of both types of fabrics were studied by scanning electron microscopy to understand the changes in the tensile properties of the fabrics. Both fabrics showed an initial well formed bond structures with an increase in bonding temperature. Both types of fabrics have shown an initial elongation and complete dissociation of the bond at low bonding temperatures. The rupture of fabrics at high

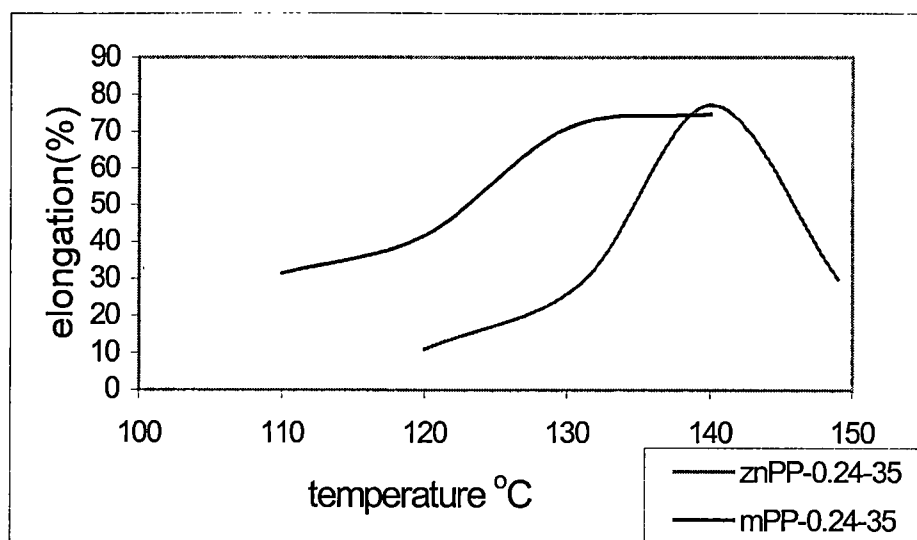


Figure 4.27. Peak strength of znPP and mPP fabrics in MD produced at 0.24 throughput rate, 35g/m² basis weight with increasing bonding temperatures.

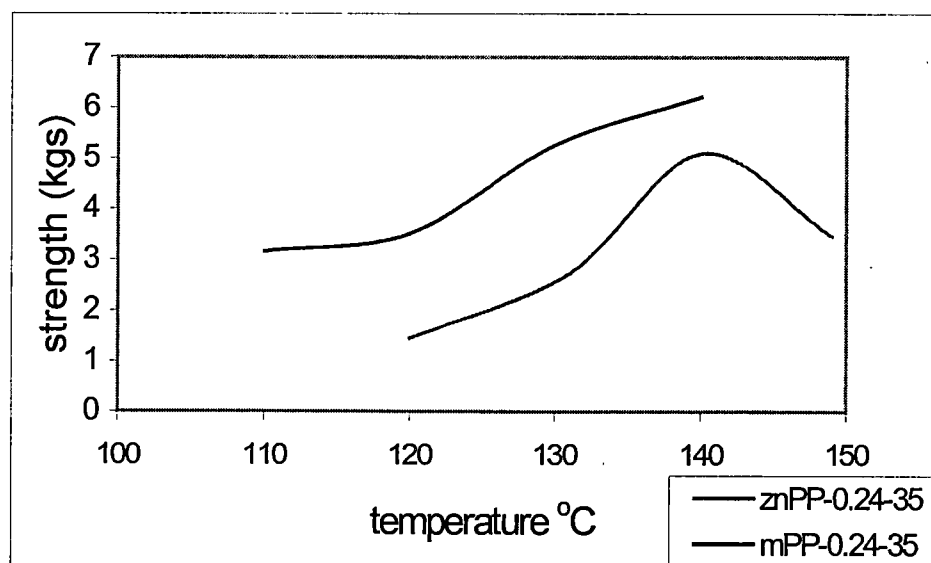


Figure 4.28. Peak elongation of znPP and mPP fabrics in MD produced at 0.24 throughput rate, 35g/m² basis weight with increasing bonding temperatures.

bonding temperatures in case of znPP was mainly due to the breakage of the filaments in the vicinity of the bond point [12], where as in case of mPP fabrics we see formation of lot of holes in the bond area, and finally the complete breakage of the bond (figure 4.26). This has to be studied further.

CHAPTER V

CONCLUSIONS

A broad range of process variables were studied to investigate the processing behavior of a mPP polymer using the Reicofil spunbonding process. The processing of mPP was almost similar to that of znPP polymer. Filament characterization showed that different extrusion and process conditions produced filaments with a range of morphology and properties. As throughput increased, the filament morphology improved, which was due to higher amount of air used to maintain the filament diameter same at all the throughputs. The mPP filaments have shown increased crystallinity, orientation, tensile strength and thermal stability with increase in throughput. The mPP filaments have also shown lower melting temperature, higher tensile strength and lower elongation compared to that of znPP filaments. The filament morphology has shown slight changes during the bonding process. This is seen by higher levels of crystallinity and crystal sizes at the bond areas and even in the unbonded areas of the fabrics. The properties of the final fabrics are the result of process conditions and the bonding conditions.

The fabrics produced with increasing throughput at constant weight required higher bonding temperatures to compensate for the reduced contact time in the nip of the calender and better developed filament morphology. Fabrics with heavier weights also required higher bonding temperatures due to increase in the material between the calender rollers. The mPP fabrics have shown similar trends to that of znPP fabrics as far as effect of weight, throughput, and bonding temperatures are concerned on the properties

of the bonded fabrics. However, mPP fabrics have also shown higher tensile strength and elongation properties than the comparable znPP fabrics.

The changes in the tensile properties of the fabrics were studied by the analysis of the mechanism of rupture. Various filament morphologies and process conditions lead to the formation of bond areas with different structures. These differences caused differences in tensile properties and in rupture mechanism. At low bonding temperatures, a complete dissociation of the bond points was observed. While at high temperatures, the breakage of the bond was observed. The mPP fabrics have shown different rupture mechanism to that of znPP fabrics and this has to be studied further. Overall, the properties of mPP fabrics were better and higher strength and elongation values were observed at relatively lower bonding temperatures.

CHAPTER VI

RECOMMENDATIONS FOR FUTURE RESEARCH

The present research has shown some interesting properties of fabrics produced over a range of process conditions. As mentioned earlier in the results, most groups of fabrics haven't shown overbonding conditions even at a temperature of 140°C based on tensile properties. This leaves a window of opportunity to carry out the process at higher bonding temperatures and study the properties. The present research also showed some interesting observations in the fabric's failure mechanism. A much-detailed study of the bond areas is recommended, to understand the exact rupture mechanisms.

With the entire data, development of computer/mathematical model to select the process conditions to achieve desired properties is very much recommended.

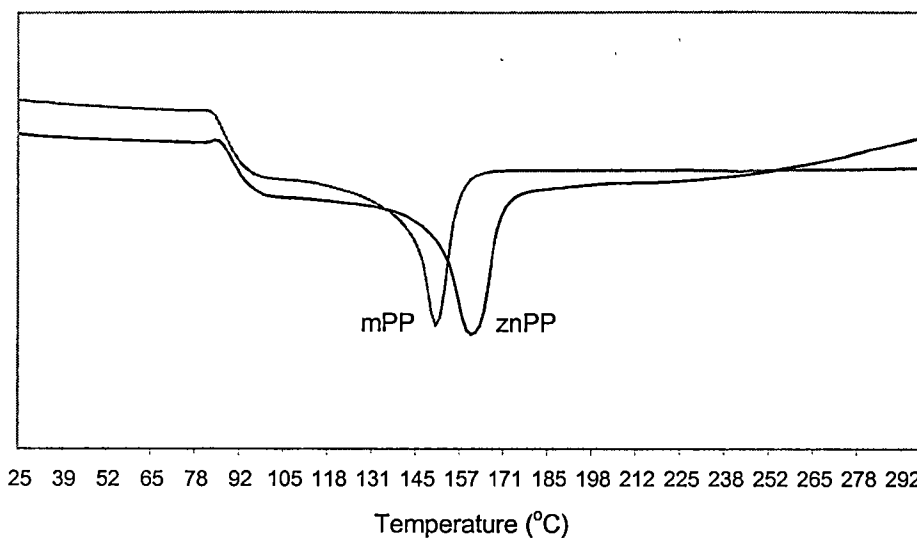
REFERENCES

1. S. R. Malkan, and L.C. Wadsworth, 'A review on Spunbond technology, Part I', *International Nonwovens Bulletin*, 03/92.
2. E. B. Bond, J.E. Spruiell, and G. Richeson, 'Conventional Ziegler-Natta Versus Metallocene Catalyzed Isotactic Polypropylene for Fiber and Nonwoven Applications.'
3. D. Permentier, C.Y. Cheng, and G.A. Stahl, 'Metallocene Based Propylene polymer for Nonwoven Applications', *Presentation at Index 96 Congress*, 02/96.
4. P. Mathews, 'Metallocene polymers, how far have they progressed?' *British Plastics & Rubber*, 03/96, p32.
5. 'Metallocene Polypropylene a first for medical spunbond fabrics', *High Performance Textiles*, 12/95.
6. 'Exxon chemical produces new plastic', *PR Newswire*, 09/95.
7. M. Eckstut, W. Kuhlke, and F. Peterson, 'Metallocene- the new wave', *Chemical Engineering*, 09/96, p92.
8. R. Nanjundappa, G. S. Bhat, and S. R. Malkan, 'Process and Property Optimization in a Spunbonding Process', *Proceedings of 9th TANDEC Conference*, Knoxville, TN 1999.
9. R. E. DeBrunner, 'The importance of bonding in Spunbond Fabrics'.
10. E. L. Wuagneux, 'Current trends and markets in Melt Blowing and Spunbonding', *Nonwovens Industry*, 11/97, p30.
11. C. W. Ericson, and J.F. Baxter, 'Spunbonded Nonwoven Fabric Studies I: Characterization of filament arrangement in the web', *Textile Research Journal*, Vol. 43, 1973.
12. D. W. Hairston, 'New Vitality for Polymerization Catalysts', *Chemical Engineering*, 08/95, p59.
13. T. F. Gilmore and R. K. Dharmadhikary, 'Thermal Point Bonding: A critical review', *INDA Journal*, Vol. 5, No. 1.
14. R. K. Dharmadhikary et al, 'Thermal bonding of Nonwoven Fabrics', *Textile Progress*, Vol. 26, No. 2.
15. R. J. Martin and G. E. R. Lamb, 'Measurement of Thermal Conductivity of Nonwovens using Dynamic Method', *Textile Research Journal*, Vol. 57, 1987.

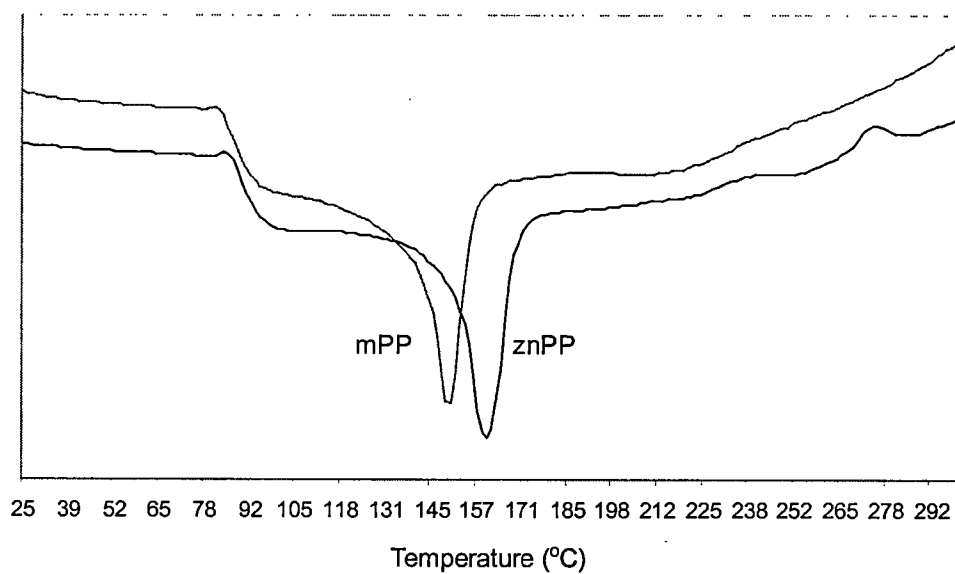
16. K. E. Duckett, and S. Kanagaraj, 'A one-dimensional finite element model to predict the temperature distribution in a thick web during thermal calendering', *INDA Journal of Nonwovens Research*, Vol. 4, No. 1, 1992.
17. V. DeAngelis, T. DiGiacchino, and P. Olivieri, 'Hot calendered Polypropylene Nonwoven fabrics', 2nd International Conference on Polypropylene Fibers and Textiles, *Plastics and Rubber Institute*, 1979.
18. S. R. Malkan, L. C. Wadsworth, and C. Davey, 'Parametric Studies of the Reicofil Spunbonding Process. Part I: Effect of Process Variables on Final Filament Diameter', *International Nonwovens Journal*, Vol. 6, No.2.
19. D. Zhang et al, 'Evolution of the Spunbonding Process. Part I: Studies with Polypropylene Homopolymer', *Journal of Applied Polymer Science*, 1996.
20. J. Chowdhury and S. Moore, 'Newsfront Polymers By Blueprint', *Chemical Engineering*, 04/93, p34.
21. S. R. Malkan, 'Advancements in Polyolefin Resins for Polymer-laid Nonwovens', *Hi-Performance Fabrics '96 Conference*, Singapore, April 24-26, 1996.
22. C. Y. Cheng et al, 'Processing Characteristics of Metallocene Propylene Homopolymer', TANDEC Conference, Knoxville, TN, 1997.
23. E. B. Bond, and J. E. Spruiell, 'Comparison of the Crystallization Behavior of Ziegler-Natta and Metallocene Catalyzed Isotactic Polypropylene', *Proceedings of 6th TANDEC Conference*, Knoxville, TN, 1996.
24. M. R. Ribero et al, 'Supported Metallocene Complex for Ethylene and Propylene Polymerization: Preparation and Activity', *Industrial Engineering Chemical Research*, Vol. 36, 1997, p1224.
25. J. Shearman, 'Chemical Polyolefins', *Chemical Engineering*, 08/92, p61.
26. P. Silverberg, 'The field widens for Single-Site Catalysts', *Chemical Engineering*, 06/97, p37.
27. Mettler Manual
28. X. C. Huang, and R. Bresee, 'Characterizing Nonwoven Web Structure using Image Analysis Techniques. Part IV: Fiber diameter analysis for Spunbonded webs', *International Nonwovens Journal*, Vol. 6, No. 4.
29. INDA Standard test 90.1 (ASTM D5732).

30. INDA Standard test 100.1 (ASTM D5734).
31. X. C. Huang and R. Bresee, 'Characterizing Nonwoven Web Structure using Image Analysis Techniques. Part II: Fiber Orientation analysis in thin webs', *Journal of Nonwovens Research*, Vol. 5, No. 2.
32. S. B. Singh, S. B. Biggers, Jr., and B. C. Goswami, 'Finite Element Modeling of the Nonuniform Deformation of Spunbonded Nonwovens', *Textile Research Journal*, Vol. 65, No. 5, 1998.

APPENDICES



Appendix 1. DSC Scans of the filaments produced at 0.35ghm.



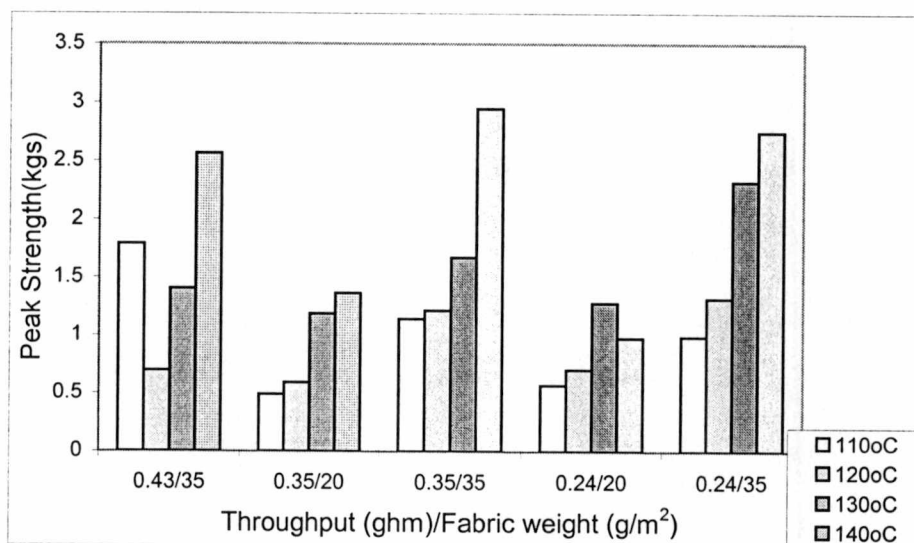
Appendix 1. DSC Scans of the filaments produced at 0.24ghm.

Sample	Throughput (ghm)	Basis weight (g/m ²)	Bond temp (°C)	Peak Strength (Kg)	Peak Extn. (%)	Yield mN/Tex	Initial Modulus N/Tex	Break Energy Kg-m
1A	0.43	35	110	0.72	35.6	7.5	0.04	0.046
2A	0.43	35	120	2.6	18.5	26.7	0.48	0.081
3A	0.43	35	130	3.35	27.9	34.7	0.47	0.115
4A	0.43	35	140	5.16	51.5	53.8	0.42	0.249
1B	0.35	20	110	1.35	19.5	25.4	0.43	0.062
2B	0.35	20	120	2.12	37.6	40.5	0.43	0.098
3B	0.35	20	130	2.94	55.1	43.2	0.37	0.144
4B	0.35	20	140	3.0	50.6	44.3	0.40	0.144
1C	0.35	35	110	2.66	22.0	28.8	0.42	0.097
2C	0.35	35	120	3.11	24.6	32.9	0.45	0.107
3C	0.35	35	130	4.17	38.9	45.7	0.44	0.177
4C	0.35	35	140	6.08	68.9	63.4	0.36	0.379
1D	0.24	20	110	2.53	55.0	47.6	0.44	0.154
2D	0.24	20	120	2.82	64.1	52.3	0.38	0.179
3D	0.24	20	130	3.45	74.0	45.0	0.37	0.235
4D	0.24	20	140	1.89	25.6	32.2	0.46	0.054
1E	0.24	35	110	3.16	31.5	34.8	0.44	0.160
2E	0.24	35	120	3.51	41.7	41.2	0.38	0.202
3E	0.24	35	130	5.26	70.9	58.9	0.40	0.367
4E	0.24	35	140	6.21	74.8	59.5	0.43	0.440

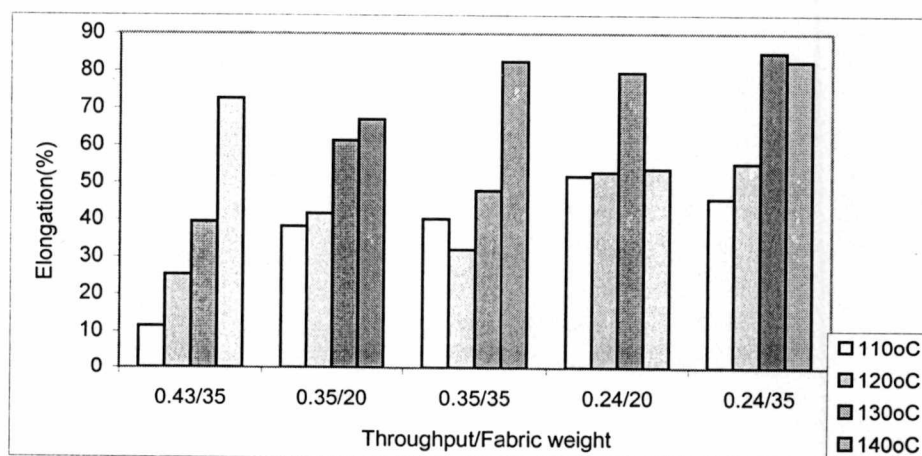
Appendix 2. Fabric tensile properties along the machine direction

Sample	Throughput (ghm)	Basis weight (g/m ²)	Bond temp (°C)	Peak Strength (Kg)	Peak Extn. (%)	Yield mN/tex	Initial Modulus N/Tex	Break Energy Kg-m
1A	0.43	35	110	1.79	11.5	19.1	0.04	0.067
2A	0.43	35	120	0.7	25.4	7.4	0.04	0.041
3A	0.43	35	130	1.40	44.5	15.4	0.05	0.078
4A	0.43	35	140	2.56	72.6	27.6	0.08	0.156
1B	0.35	20	110	0.49	38.3	9.0	0.05	0.029
2B	0.35	20	120	0.59	62.1	11.1	0.06	0.042
3B	0.35	20	130	1.19	61.4	22.0	0.07	0.069
4B	0.35	20	140	1.37	67.0	25.9	0.06	0.075
1C	0.35	35	110	1.14	40.4	11.3	0.09	0.067
2C	0.35	35	120	1.21	32.2	13.0	0.12	0.068
3C	0.35	35	130	1.67	48.0	18.4	0.10	0.097
4C	0.35	35	140	2.95	82.6	33.0	0.08	0.197
1D	0.24	20	110	0.57	51.8	10.4	0.04	0.041
2D	0.24	20	120	0.71	52.9	13.4	0.05	0.044
3D	0.24	20	130	1.28	79.7	24.8	0.05	0.086
4D	0.24	20	140	0.98	53.8	17.6	0.07	0.045
1E	0.24	35	110	0.99	45.7	10.9	0.09	0.072
2E	0.24	35	120	1.32	55.3	14.7	0.09	0.103
3E	0.24	35	130	2.32	84.9	25.7	0.07	0.180
4E	0.24	35	140	2.75	82.6	29.2	0.08	0.191

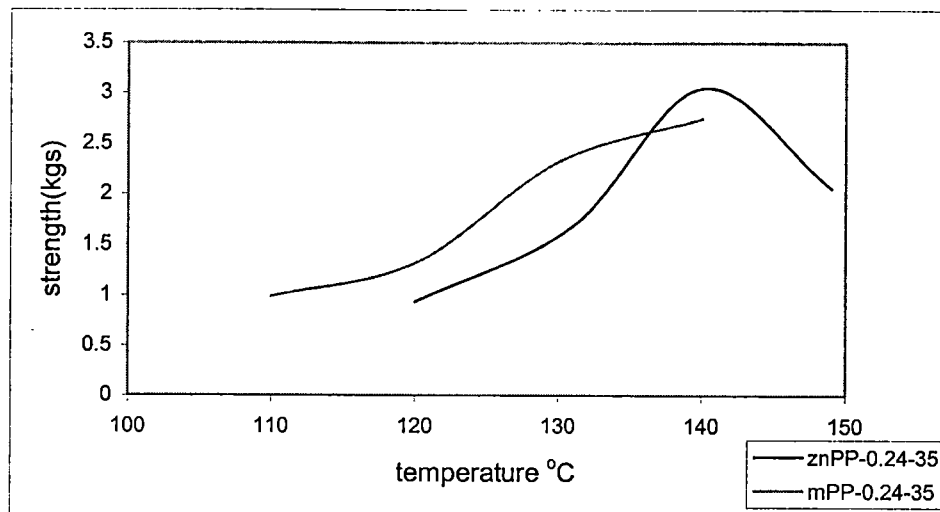
Appendix 2. Fabric tensile properties along the cross direction



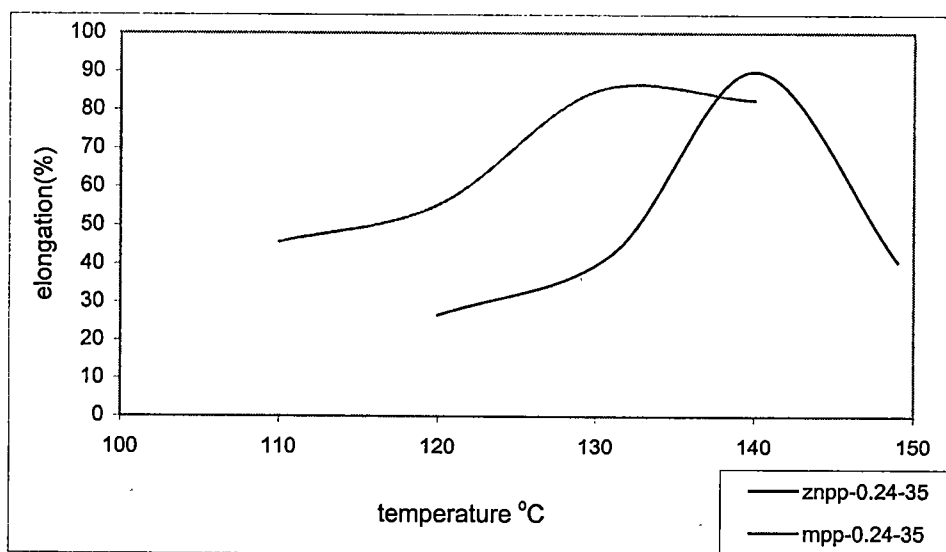
Appendix 2. Peak Strength in CD with increasing bonding temperatures.



Appendix 2. Peak Elongation in CD with increasing bonding temperatures.



Appendix 2. Peak strength of znPP and mPP fabrics in CD produced at 0.24 throughput rate, 35g/m² fabric weight with increasing bonding temperatures.



Appendix 2. Peak Elongation of znPP and mPP fabrics in CD produced at 0.24 throughput rate, 35g/m² fabric weight with increasing bonding temperatures.

VITA

Ramaiah Kotra was born in Tadpatri, India on 7th August 1975. He attended schools at Sri Aurobindo Centenary School, Tadpatri, and A.P.R.J.C Junior College, Nimmakur, India. He joined Bapuji Institute of Engineering & Technology in Davangere, India and received a degree in Bachelor of Technology in Textile Technology in 1997. He worked in India for one and half years and then joined the Master's program in Textile Science at the University of Tennessee, Knoxville. He was employed as a Graduate Research Assistant at the University of Tennessee from Fall 1999 to Fall 2000. He graduated in May 2001 and presently working at Oracle Corporation, Atlanta, GA.